

Quantum parameter estimation on coherently superposed noisy channels

François CHAPEAU-BLONDEAU,

Laboratoire Angevin de Recherche en Ingénierie des Systèmes (LARIS),
Université d'Angers, 62 avenue Notre Dame du Lac, 49000 Angers, France.

October 14, 2021

Abstract

A generic qubit unitary operator affected by quantum noise is duplicated and inserted in a coherently superposed channel, superposing two paths offered to a probe qubit across the noisy unitary, and driven by a control qubit. A characterization is performed of the transformation realized by the superposed channel on the joint state of the probe-control qubit pair. The superposed channel is then specifically analyzed for the fundamental metrological task of phase estimation on the noisy unitary, with the performance assessed by the Fisher information, classical or quantum. A comparison is made with conventional estimation techniques and also with a quantum switched channel with indefinite causal order recently investigated for a similar task of phase estimation. In the analysis here, a first important observation is that the control qubit of the superposed channel, although it never directly interacts with the unitary being estimated, can nevertheless be measured alone for effective estimation, while discarding the probe qubit that interacts with the unitary. This property is also present with the switched channel but is inaccessible with conventional techniques. The optimal measurement of the control qubit here is characterized in general conditions. A second important observation is that the noise plays an essential role in coupling the control qubit to the unitary, and that the control qubit remains operative for phase estimation at very strong noise, even with a fully depolarizing noise, whereas conventional estimation and the switched channel become inoperative in these conditions. The results extend the analysis of the capabilities of coherently controlled channels which represent novel devices exploitable for quantum signal and information processing.

1 Introduction

Quantum channels, when exploited for information processing, can be combined in specifically quantum ways, that differ from standard classical combinations, and that offer novel capabilities with no classical analogue. Such techniques have been recently introduced, and two basic and prominent examples of them are the switch of two quantum channels in indefinite causal order, and the coherent superposition of two quantum channels. These two basic schemes combine two quantum channels (1) and (2) and operate in the following manner.

The first scheme (the switched channel) [1, 2, 3] uses a quantum switch driven by a control qubit to select between cascading the two channels in the order (1)–(2) or (2)–(1). When the control

Preprint of a paper published by *Physical Review A*, vol. 104, 032214, pp. 1–16 (2021).

<https://doi.org/10.1103/PhysRevA.104.032214>

<https://journals.aps.org/pra/abstract/10.1103/PhysRevA.104.032214>

qubit is placed in a superposed state, the two individual channels become cascaded in a superposition of the two classical orders (1)–(2) and (2)–(1), realizing a switched quantum channel incorporating simultaneously the two alternative orders, or with indefinite causal order.

The second scheme (the superposed channel) [4, 5, 6] uses a control qubit to drive an information-carrying or signal quantum state either across channel (1) or across channel (2). When the control qubit is placed in a superposed state, the scheme realizes a coherently superposed channel offering a coherent superposition of the two alternative paths across (1) and (2).

Both schemes are specifically quantum devices, and represent novel resources exploitable for quantum information processing [5, 6]. The main area where these novel techniques have been analyzed and compared is quantum communication. A typical and striking benefit is when the two channels (1) and (2) are two completely depolarizing quantum channels, which are therefore individually incapable of transmitting any useful information. It has then been shown that when two such channels are associated into a switched channel with indefinite order [3, 7], or into a coherently superposed channel [4, 7], in each scheme effective information communication becomes possible. Comparison has been performed and discussed [4, 7, 8] to better appreciate the mechanisms and specificities of the two schemes, and the respective roles of indefinite order and of coherent superposition, particularly in reaching similar capabilities of information communication through depolarizing channels.

More recently, switched channels with indefinite order have been investigated in another important information-processing task, for quantum metrology, consisting in phase estimation from a noisy unitary transformation [9]. Specific capabilities, useful to estimation, have been reported and analyzed in the switched channels, for example the possibility of using a completely depolarized input signal as an operative probe for estimation (while this is never possible with conventional techniques).

As a complement to [9], we will investigate a comparable scenario of phase estimation from a noisy unitary, when undertaken here by means of a coherently superposed channel. The study will bring additional results on the capabilities of coherently superposed channels for quantum information processing, along with more elements of comparison between the two schemes of switched indefinite order and of coherently superposed channels.

2 Coherent superposition of two quantum channels

We consider as in [4, 5, 6], acting on quantum systems with Hilbert space \mathcal{H} , a quantum channel (1) with K_1 Kraus operators $K_j^{(1)} \in \mathcal{L}(\mathcal{H})$ for $j = 1$ to K_1 , and a second quantum channel (2) with K_2 Kraus operators $K_k^{(2)} \in \mathcal{L}(\mathcal{H})$ for $k = 1$ to K_2 . A quantum system with density operator $\rho \in \mathcal{L}(\mathcal{H})$ acting as an input signal can be sent across either channel (1) or channel (2), according to the state of a control qubit with two-dimensional Hilbert space \mathcal{H}_2 referred to the orthonormal basis $\{|0_c\rangle, |1_c\rangle\}$. When the control qubit is in state $|0_c\rangle$ the input signal ρ is sent across channel (1), and when the control qubit is in state $|1_c\rangle$ the input signal ρ is sent across channel (2). The resulting quantum superposed channel is depicted in Fig. 1.

In this study, the coherently superposed channel of Fig. 1 will superpose two noisy unitary channels to be involved in a task of quantum parameter estimation, the same task considered in [9] in a switched channel with indefinite causal order. Before we come to this, the operation of the coherently superposed channel of Fig. 1 needs to be more completely defined, especially for an arbitrary state ρ_c of the control qubit. For this purpose, following [4], we will rely on a Stinespring dilation for the superposed channel of Fig. 1, involving a description of the interaction with the surrounding environment underlying the operation of the superposed channel.

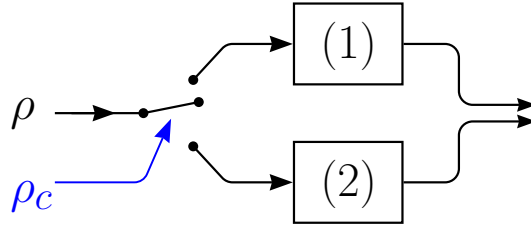


Figure 1: A quantum state ρ as an input signal can be sent across either channel (1) or channel (2), according to the state ρ_c of a control qubit.

The compound signal-control-environment, with a control qubit in state $|0_c\rangle$ evolves unitarily as

$$|\psi\rangle \otimes |0_c\rangle \otimes |g^{(1)}\rangle \otimes |g^{(2)}\rangle \mapsto \sum_{j=1}^{K_1} K_j^{(1)} |\psi\rangle \otimes |0_c\rangle \otimes |e_j^{(1)}\rangle \otimes |g^{(2)}\rangle, \quad (1)$$

and with a control qubit in state $|1_c\rangle$ it evolves unitarily as

$$|\psi\rangle \otimes |1_c\rangle \otimes |g^{(1)}\rangle \otimes |g^{(2)}\rangle \mapsto \sum_{k=1}^{K_2} K_k^{(2)} |\psi\rangle \otimes |1_c\rangle \otimes |g^{(1)}\rangle \otimes |e_k^{(2)}\rangle, \quad (2)$$

for any signal state $|\psi\rangle \in \mathcal{H}$, and where we have introduced for channel (1) with K_1 Kraus operators a K_1 -dimensional environment E_1 of orthonormal basis $\{|e_j^{(1)}\rangle\}_{j=1}^{K_1}$ initialized in state $|g^{(1)}\rangle$, and for channel (2) with K_2 Kraus operators a K_2 -dimensional environment E_2 of orthonormal basis $\{|e_k^{(2)}\rangle\}_{k=1}^{K_2}$ initialized in state $|g^{(2)}\rangle$. In practice, a controlled operation like in Eqs. (1)–(2), can be carried out by an interferometric setup, such as those discussed in [10, 11, 4], with for instance the control realized by the polarization of a photon and the signal state $|\psi\rangle$ by other degrees of freedom such as quantum spatial modes of the same photon.

An arbitrary state ρ_c of the control qubit is defined as a linear combination of the four matrix elements $|0_c\rangle\langle 0_c|$, $|0_c\rangle\langle 1_c|$, $|1_c\rangle\langle 0_c|$ and $|1_c\rangle\langle 1_c|$, and in such circumstance the corresponding evolution of the compound signal-control-environment follows by linearity of Eqs. (1)–(2). For instance, for the control $|0_c\rangle\langle 0_c|$ we have from Eq. (1),

$$|\psi\rangle\langle\psi| \otimes |0_c\rangle\langle 0_c| \otimes |g^{(1)}\rangle\langle g^{(1)}| \otimes |g^{(2)}\rangle\langle g^{(2)}| \mapsto \sum_{j=1}^{K_1} \sum_{j'=1}^{K_1} K_j^{(1)} |\psi\rangle\langle\psi| K_{j'}^{(1)\dagger} \otimes |0_c\rangle\langle 0_c| \otimes |e_j^{(1)}\rangle\langle e_{j'}^{(1)}| \otimes |g^{(2)}\rangle\langle g^{(2)}|, \quad (3)$$

which upon partial tracing over the two environments via $\text{tr}_{E_1 E_2}(\cdot)$ leads to the non-unitary evolution of the signal-control compound as

$$|\psi\rangle\langle\psi| \otimes |0_c\rangle\langle 0_c| \mapsto \sum_{j=1}^{K_1} K_j^{(1)} |\psi\rangle\langle\psi| K_j^{(1)\dagger} \otimes |0_c\rangle\langle 0_c|, \quad (4)$$

where we recognize for the signal state $|\psi\rangle\langle\psi|$ the evolution induced by channel (1) alone. In a similar way, the evolution with the control $|1_c\rangle\langle 1_c|$ and Eq. (2) leads to

$$|\psi\rangle\langle\psi| \otimes |1_c\rangle\langle 1_c| \mapsto \sum_{k=1}^{K_2} K_k^{(2)} |\psi\rangle\langle\psi| K_k^{(2)\dagger} \otimes |1_c\rangle\langle 1_c|, \quad (5)$$

where we recognize for the signal state $|\psi\rangle\langle\psi|$ the evolution induced by channel (2) alone.

With the control $|0_c\rangle\langle 1_c|$ we have from Eqs. (1) and (2),

$$|\psi\rangle\langle\psi|\otimes|0_c\rangle\langle 1_c|\otimes|g^{(1)}\rangle\langle g^{(1)}|\otimes|g^{(2)}\rangle\langle g^{(2)}| \mapsto \sum_{j=1}^{K_1} \sum_{k=1}^{K_2} \mathsf{K}_j^{(1)} |\psi\rangle\langle\psi| \mathsf{K}_k^{(2)\dagger} \otimes |0_c\rangle\langle 1_c| \otimes |e_j^{(1)}\rangle\langle e_0^{(1)}|\otimes|g^{(2)}\rangle\langle e_k^{(2)}|, \quad (6)$$

which by partial tracing over the two environments $E_1 E_2$ leads for the signal-control compound to the transformed state

$$\left(\sum_{j=1}^{K_1} \langle g^{(1)}|e_j^{(1)}\rangle \mathsf{K}_j^{(1)} \right) |\psi\rangle\langle\psi| \left(\sum_{k=1}^{K_2} \langle e_k^{(2)}|g^{(2)}\rangle \mathsf{K}_k^{(2)\dagger} \right) \otimes |0_c\rangle\langle 1_c| = \mathsf{T}_1 |\psi\rangle\langle\psi| \mathsf{T}_2^\dagger \otimes |0_c\rangle\langle 1_c|, \quad (7)$$

where we have defined the two operators of $\mathcal{L}(\mathcal{H})$,

$$\mathsf{T}_1 = \sum_{j=1}^{K_1} \langle g^{(1)}|e_j^{(1)}\rangle \mathsf{K}_j^{(1)}, \quad (8)$$

$$\mathsf{T}_2 = \sum_{k=1}^{K_2} \langle g^{(2)}|e_k^{(2)}\rangle \mathsf{K}_k^{(2)}, \quad (9)$$

that are the two transformation operators introduced in [4]. The operators T_1 and T_2 of Eqs. (8)–(9) appear as essential to the operation of the superposed channel of Fig. 1. The two operators T_1 and T_2 , as visible in Eqs. (8)–(9), depend on the environment models for implementing channels (1) and (2), especially via the initial states $|g^{(1)}\rangle$ and $|g^{(2)}\rangle$. This is the same observation as in [4], that the Kraus operators $\{\mathsf{K}_j^{(1)}\}_{j=1}^{K_1}$ and $\{\mathsf{K}_k^{(2)}\}_{k=1}^{K_2}$ alone, (unlike the situation of the switched channel of [1, 2, 3, 9]), are not sufficient to precisely specify the operation of the superposed channel of Fig. 1, but that a reference to a specific implementation of each channel via an environment model is necessary. We will discuss further these specific aspects related to the underlying channel implementation and relevant to the superposed channel, in particular in Section 6.4 and in the Appendix. Now we proceed in the analysis of the coherently superposed channel.

For an arbitrary input signal state $\rho \in \mathcal{L}(\mathcal{H})$, which is a convex sum of pure states like $|\psi\rangle\langle\psi|$, and an arbitrary state $\rho_c \in \mathcal{L}(\mathcal{H}_2)$ for the control qubit, we consequently obtain by linearity of the evolution, the quantum operation realized on the signal-control compound by the coherently superposed channel of Fig. 1, as

$$\begin{aligned} \mathcal{S}(\rho \otimes \rho_c) &= \mathcal{S}_{00}(\rho) \otimes \langle 0_c|\rho_c|0_c\rangle |0_c\rangle\langle 0_c| + \mathcal{S}_{01}(\rho) \otimes \langle 0_c|\rho_c|1_c\rangle |0_c\rangle\langle 1_c| \\ &+ \mathcal{S}_{01}^\dagger(\rho) \otimes \langle 1_c|\rho_c|0_c\rangle |1_c\rangle\langle 0_c| + \mathcal{S}_{11}(\rho) \otimes \langle 1_c|\rho_c|1_c\rangle |1_c\rangle\langle 1_c|, \end{aligned} \quad (10)$$

with the superoperators

$$\mathcal{S}_{00}(\rho) = \sum_{j=1}^{K_1} \mathsf{K}_j^{(1)} \rho \mathsf{K}_j^{(1)\dagger}, \quad (11)$$

$$\mathcal{S}_{11}(\rho) = \sum_{k=1}^{K_2} \mathsf{K}_k^{(2)} \rho \mathsf{K}_k^{(2)\dagger}, \quad (12)$$

$$\mathcal{S}_{01}(\rho) = \mathsf{T}_1 \rho \mathsf{T}_2^\dagger. \quad (13)$$

The superoperator $\mathcal{S}_{00}(\rho)$ describes the quantum operation realized by channel (1) alone, and similarly with $\mathcal{S}_{11}(\rho)$ for channel (2). The superoperator $\mathcal{S}_{01}(\rho)$ is an interference term manifesting the coherent superposition of channels (1) and (2) in Fig. 1. In the joint state $\mathcal{S}(\rho \otimes \rho_c)$ of Eq. (10),

if the control qubit were discarded (unobserved) and traced out, the resulting quantum operation on ρ would reduce to $\rho \mapsto \mathcal{S}_{00}(\rho) \langle 0_c | \rho_c | 0_c \rangle + \mathcal{S}_{11}(\rho) \langle 1_c | \rho_c | 1_c \rangle$, representing a classical probabilistic (convex) combination of the channels (1) and (2) traversed with respective probabilities $\langle 0_c | \rho_c | 0_c \rangle$ and $\langle 1_c | \rho_c | 1_c \rangle$. By contrast, if the control qubit is treated coherently with ρ , it can give rise to specific, specifically quantum, behaviors from the superposed channel, as we are going to see.

An interesting and specifically quantum feature is that the control qubit can be placed in the superposed state $|\psi_c\rangle = \sqrt{p_c}|0_c\rangle + \sqrt{1-p_c}|1_c\rangle$, with $p_c \in [0, 1]$. This produces in Fig. 1 a quantum superposed channel representing a coherent superposition of two alternative paths for ρ across channel (1) and channel (2) simultaneously. With $\rho_c = |\psi_c\rangle\langle\psi_c|$, the quantum operation resulting from Eq. (10) takes the form

$$\begin{aligned} \mathcal{S}(\rho \otimes \rho_c) &= p_c \mathcal{S}_{00}(\rho) \otimes |0_c\rangle\langle 0_c| + (1-p_c) \mathcal{S}_{11}(\rho) \otimes |1_c\rangle\langle 1_c| \\ &+ \sqrt{(1-p_c)p_c} \left[\mathcal{S}_{01}(\rho) \otimes |0_c\rangle\langle 1_c| + \mathcal{S}_{01}^\dagger(\rho) \otimes |1_c\rangle\langle 0_c| \right]. \end{aligned} \quad (14)$$

This description of the operation of the coherently superposed channel of Fig. 1 applies when (1) and (2) are two arbitrary quantum channels. We will now consider the situation as in [9], where the quantum channels (1) and (2) are qubit channels, under a form which is often encountered in quantum metrology, and consisting in a unitary operator U_ξ affected by a quantum noise $\mathcal{N}(\cdot)$.

3 A qubit unitary channel with noise

When channels (1) and (2) in Fig. 1 are qubit channels, an interesting feature is that the two transformation operators T_1 and T_2 of Eqs. (8) and (9), are operators of $\mathcal{L}(\mathcal{H}_2)$ which can be conveniently characterized in Bloch representation, i.e. in the basis of the four Pauli operators $\{I_2, \sigma_x, \sigma_y, \sigma_z\}$ forming an orthogonal basis for the operator space $\mathcal{L}(\mathcal{H}_2)$. The Bloch representation for T_1 and T_2 will originate in their respective set of Kraus operators and underlying environment models appearing in Eqs. (8) and (9), but will generally involve no more than four coordinates, for each operator T_1 or T_2 , in the Pauli basis. This will usually enable a concise characterization in Bloch representation of the superoperator $\mathcal{S}_{01}(\rho)$ of Eq. (13) that conveys the coupling and effects specific to the coherently superposed channel. This approach, in its generality for qubit channels, will be presented here in the interesting case where each channel (1) and (2) is a unitary qubit channel affected by a generic qubit noise.

For qubits with two-dimensional Hilbert space \mathcal{H}_2 , the density operator is represented in Bloch representation [12] under the form

$$\rho = \frac{1}{2}(\mathbb{I}_2 + \vec{r} \cdot \vec{\sigma}), \quad (15)$$

where \mathbb{I}_2 is the identity operator on \mathcal{H}_2 , and $\vec{\sigma}$ a formal vector assembling the three (traceless Hermitian unitary) Pauli operators $[\sigma_x, \sigma_y, \sigma_z] = \vec{\sigma}$. The Bloch vector $\vec{r} \in \mathbb{R}^3$ characterizing the density operator has norm $\|\vec{r}\| = 1$ for a pure state, and $\|\vec{r}\| < 1$ for a mixed state.

A qubit unitary operator U_ξ is introduced with the general parameterization [12]

$$U_\xi = \exp\left(-i\frac{\xi}{2}\vec{n} \cdot \vec{\sigma}\right), \quad (16)$$

where $\vec{n} = [n_x, n_y, n_z]^T$ is a unit vector of \mathbb{R}^3 , and ξ a phase angle in $[0, 2\pi)$. Such an U_ξ represents for instance the transformation of a photon polarization by an optical interferometer, with the axis \vec{n} fixed by the orientation of the polarizing beam splitter and a phase shift ξ occurring between the two

arms of the interferometer. From a qubit state ρ in Bloch representation as in Eq. (15), the unitary U_ξ produces the transformed state

$$U_\xi \rho U_\xi^\dagger = \frac{1}{2}(\mathbb{I}_2 + U_\xi \vec{r} \cdot \vec{\sigma}), \quad (17)$$

where U_ξ is the 3×3 real matrix² representing in \mathbb{R}^3 the rotation around the axis \vec{n} by the angle ξ .

A qubit noise $\mathcal{N}(\cdot)$ is also introduced, implementing a quantum operation which is represented [12] by the Kraus operators Λ_j of $\mathcal{L}(\mathcal{H}_2)$, which need not be more than four for representing any qubit noise. Equivalently, the transformation $\rho \mapsto \mathcal{N}(\rho)$ by the qubit noise can be defined [12] by the affine transformation of the qubit Bloch vector

$$\vec{r} \mapsto A\vec{r} + \vec{c}, \quad (18)$$

mapping the unit Bloch ball into itself, and characterized by the 3×3 real matrix A and vector $\vec{c} \in \mathbb{R}^3$.

Each quantum channel like (1) or (2) of Section 2 is formed by cascading the unitary transformation U_ξ of Eq. (16) and the general qubit noise $\mathcal{N}(\cdot)$ of Eq. (18), as depicted in Fig. 2.

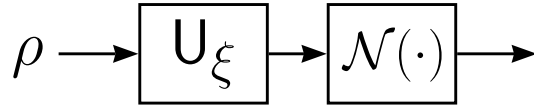


Figure 2: A qubit channel formed by the unitary transformation U_ξ of Eq. (16) and the general qubit noise $\mathcal{N}(\cdot)$ of Eq. (18). As a whole this channel is an instance of channel (1) or (2) considered in Fig. 1.

For the quantum channel of Fig. 2, the Kraus operators like $K_j^{(1)}$ or $K_k^{(2)}$ of Section 2 result as $K_j = \Lambda_j U_\xi$. Equivalently, for a qubit state ρ in Bloch representation as in Eq. (15), the cascade of U_ξ then $\mathcal{N}(\cdot)$ produces the transformed state

$$\mathcal{N}(U_\xi \rho U_\xi^\dagger) = \frac{1}{2}[\mathbb{I}_2 + (AU_\xi \vec{r} + \vec{c}) \cdot \vec{\sigma}]. \quad (19)$$

4 Coherent superposition of two noisy unitaries

Two identical qubit channels formed by U_ξ and $\mathcal{N}(\cdot)$ as in Fig. 2 are associated as in Fig. 1 through the coherent quantum superposition of Section 2, with however two independent sources of a same type of qubit noise $\mathcal{N}(\cdot)$ according to Eq. (18). For two such identical channels (1) and (2), one has $\mathcal{S}_{00}(\rho) = \mathcal{S}_{11}(\rho)$ in Eqs. (11)–(12), and also $\mathcal{S}_{01}^\dagger(\rho) = \mathcal{S}_{01}(\rho)$ in Eq. (13). On the probe qubit in state ρ and control qubit in state $\rho_c = |\psi_c\rangle\langle\psi_c|$, the coherently superposed channel therefore realizes the two-qubit quantum operation from Eq. (14) reading

$$\begin{aligned} \mathcal{S}(\rho \otimes \rho_c) &= \mathcal{S}_{00}(\rho) \otimes [p_c |0_c\rangle\langle 0_c| + (1 - p_c) |1_c\rangle\langle 1_c|] \\ &+ \mathcal{S}_{01}(\rho) \otimes \sqrt{(1 - p_c)p_c} (|0_c\rangle\langle 1_c| + |1_c\rangle\langle 0_c|). \end{aligned} \quad (20)$$

As already mentioned, the superoperator $\mathcal{S}_{00}(\rho)$ (and $\mathcal{S}_{11}(\rho)$ similarly) describes the quantum operation realized on ρ by directly traversing the noisy unitary channel of Fig. 2, and it is given in Bloch representation by Eq. (19) as

$$\mathcal{S}_{00}(\rho) = \frac{1}{2}[\mathbb{I}_2 + (AU_\xi \vec{r} + \vec{c}) \cdot \vec{\sigma}]. \quad (21)$$

²We use the notation U_ξ in upright font for the unitary operator acting in the complex Hilbert space \mathcal{H}_2 of the qubit; while we use the notation U_ξ in italic font for the real matrix expressing the action of the unitary operator in the Bloch representation of qubit states in \mathbb{R}^3 .

In the superoperator $\mathcal{S}_{01}(\rho)$ of Eq. (13), for two identical channels (1) and (2) with the same set of Kraus operators $K_j = \Lambda_j U_\xi$, the two transformation operators T_1 and T_2 of Eqs. (8)–(9) have the same form, and they can be expressed as $T_1 = T_2 = T U_\xi$, with the operator of $\mathcal{L}(\mathcal{H}_2)$,

$$T = \sum_j \langle g|e_j\rangle \Lambda_j, \quad (22)$$

where $\{|e_j\rangle\}$ is the reference basis for each of the two identical environment models initialized in state $|g\rangle$. As we announced at the beginning of Section 3, it is generally possible to represent the operator $T \in \mathcal{L}(\mathcal{H}_2)$ in the Pauli basis with the Bloch representation

$$T = t_0 I_2 + \vec{t} \cdot \vec{\sigma}, \quad (23)$$

with the four complex coordinates t_0 and $\vec{t} = [t_x, t_y, t_z]^\top$. For example, for the class of Pauli noises [12, 13] the four Kraus operators $\{\Lambda_j\}$ are $\{\sqrt{p_0}I_2, \sqrt{p_x}\sigma_x, \sqrt{p_y}\sigma_y, \sqrt{p_z}\sigma_z\}$ with $\{p_j\}$ a probability distribution. This class of Pauli noises acts through random applications of the four Pauli operators, and it contains in particular such important noises as the bit-flip, the phase-flip, the bit-phase-flip, the depolarizing noises. The corresponding Bloch coordinates for T in Eq. (23) are $t_0 = \langle g|e_1\rangle \sqrt{p_0}$ and $\vec{t} = [\langle g|e_2\rangle \sqrt{p_x}, \langle g|e_3\rangle \sqrt{p_y}, \langle g|e_4\rangle \sqrt{p_z}]^\top$.

It is now possible to characterize the action of the superoperator $\mathcal{S}_{01}(\rho)$ of Eq. (13) in Bloch representation, starting with

$$\mathcal{S}_{01}(\rho) = \frac{1}{2}\mathcal{S}_{01}(I_2) + \frac{1}{2}\mathcal{S}_{01}(\vec{r} \cdot \vec{\sigma}) = T U_\xi \rho U_\xi^\dagger T^\dagger. \quad (24)$$

To proceed, we will need the identity $(\vec{a} \cdot \vec{\sigma})(\vec{b} \cdot \vec{\sigma}) = (\vec{a} \cdot \vec{b}) I_2 + i(\vec{a} \times \vec{b}) \cdot \vec{\sigma}$ for any two vectors \vec{a} and \vec{b} of \mathbb{C}^3 . As a next step, we can evaluate $\mathcal{S}_{01}(I_2) = T T^\dagger = (t_0 I_2 + \vec{t} \cdot \vec{\sigma})(t_0^* I_2 + \vec{t}^* \cdot \vec{\sigma})$ which, by the previous identity is

$$\mathcal{S}_{01}(I_2) = (t_0 t_0^* + \vec{t} \cdot \vec{t}^*) I_2 + (t_0^* \vec{t} + t_0 \vec{t}^* + i\vec{t} \times \vec{t}^*) \cdot \vec{\sigma}. \quad (25)$$

Next, it is convenient to evaluate, for a generic Bloch vector \vec{r} , the operator $T(\vec{r} \cdot \vec{\sigma})T^\dagger$, as a useful step toward obtaining $\mathcal{S}_{01}(\vec{r} \cdot \vec{\sigma}) = T(U_\xi \vec{r} \cdot \vec{\sigma})T^\dagger$. As for $\mathcal{S}_{01}(I_2)$, by performing the (non-commutative) products of Pauli operators, we obtain

$$\begin{aligned} T(\vec{r} \cdot \vec{\sigma})T^\dagger &= [(t_0^* \vec{t} + t_0 \vec{t}^* + i\vec{t}^* \times \vec{t}) \vec{r}] I_2 \\ &+ [(\vec{t} \cdot \vec{r}) \vec{t}^* + (\vec{t}^* \cdot \vec{r}) \vec{t} + (t_0 t_0^* - \vec{t} \cdot \vec{t}^*) \vec{r} + i(t_0^* \vec{t} - t_0 \vec{t}^*) \times \vec{r}] \cdot \vec{\sigma}. \end{aligned} \quad (26)$$

It can be verified that the Bloch representations in Eqs. (25) and (26) have real coordinates in the Pauli basis, as it should since $\mathcal{S}_{01}(\rho)$ here is Hermitian. For a more concise notation, Eq. (26) can be conveniently rewritten as

$$T(\vec{r} \cdot \vec{\sigma})T^\dagger = (\vec{s} \cdot \vec{r}) I_2 + A_t \vec{r} \cdot \vec{\sigma}. \quad (27)$$

In Eq. (27) has been introduced the 3×3 real matrix A_t function of t_0 and \vec{t} , and defined from Eq. (26) by the factor of $\vec{\sigma}$ which is a real linear function of \vec{r} . In Eq. (27), we have also introduced the real vector

$$\vec{s} = t_0^* \vec{t} + t_0 \vec{t}^* + i\vec{t}^* \times \vec{t} = 2 \Re(t_0^* \vec{t}) + i\vec{t}^* \times \vec{t} \quad (28)$$

of \mathbb{R}^3 , which is real since $i\vec{t}^* \times \vec{t} = (i\vec{t}^* \times \vec{t})^*$ is real. We then deduce

$$\mathcal{S}_{01}(\vec{r} \cdot \vec{\sigma}) = T(U_\xi \vec{r} \cdot \vec{\sigma})T^\dagger = (\vec{s} U_\xi \vec{r}) I_2 + A_t U_\xi \vec{r} \cdot \vec{\sigma}. \quad (29)$$

By combining Eqs. (25) and (29) we now obtain a characterization for Eq. (24) in Bloch representation as

$$\mathcal{S}_{01}(\rho) = \frac{1}{2}(t_0 t_0^* + \vec{t} \vec{t}^* + \vec{s} U_\xi \vec{r}) \mathbf{I}_2 + \frac{1}{2}(t_0^* \vec{t} + t_0 \vec{t}^* + i \vec{t} \times \vec{t}^* + A_t U_\xi \vec{r}) \cdot \vec{\sigma}. \quad (30)$$

Equations (30) and (21) in Bloch representation now provide a characterization for the joint two-qubit state $\mathcal{S}(\rho \otimes \rho_c)$ of Eq. (20) produced by the coherently superposed channel.

We will now examine how quantum measurement on the joint state $\mathcal{S}(\rho \otimes \rho_c)$ of Eq. (20) produced by the superposed channel, allows us to obtain useful information about the unitary U_ξ . This will serve to the analysis of the superposed channel for a task of parameter estimation on the unitary U_ξ , the same task investigated in [9] in a switched channel with indefinite causal order.

5 Measurement

The probe qubit prepared in state ρ and the control qubit prepared in state ρ_c get coupled by the operation of the coherently superposed quantum channel, and these two qubits together terminate in the joint state $\mathcal{S}(\rho \otimes \rho_c)$ of Eq. (20). To extract information from the superposed channel, a useful strategy, also adopted for instance in [3, 9], is to measure the control qubit in the Fourier basis $\{|+\rangle, |-\rangle\}$ of \mathcal{H}_2 . The measurement can be described by the two measurement operators $\{I_2 \otimes |+\rangle\langle +|, I_2 \otimes |-\rangle\langle -|\}$ acting in the Hilbert space $\mathcal{H}_2 \otimes \mathcal{H}_2$ of the probe-control qubit pair with state $\mathcal{S}(\rho \otimes \rho_c)$. The measurement randomly projects the control qubit either in state $|+\rangle$ or $|-\rangle$, and it leaves the probe qubit in the unnormalized conditional state

$$\rho_\pm = {}_c\langle \pm | \mathcal{S}(\rho \otimes \rho_c) | \pm \rangle_c = \frac{1}{2} \mathcal{S}_{00}(\rho) \pm \sqrt{(1-p_c)p_c} \mathcal{S}_{01}(\rho), \quad (31)$$

the partial products involving $|\pm\rangle_c$ being defined on the control qubit. The probabilities P_\pm^{con} of the two measurement outcomes are provided by the trace $P_\pm^{\text{con}} = \text{tr}(\rho_\pm)$. From Eq. (21) we have $\text{tr}[\mathcal{S}_{00}(\rho)] = 1$, and by applying the trace on Eq. (30) we obtain

$$P_\pm^{\text{con}} = \text{tr}(\rho_\pm) = \frac{1}{2} \pm \sqrt{(1-p_c)p_c} Q_\xi, \quad (32)$$

with the real scalar factor

$$Q_\xi = \text{tr}[\mathcal{S}_{01}(\rho)] = t_0 t_0^* + \vec{t} \vec{t}^* + \vec{s} U_\xi \vec{r}. \quad (33)$$

This provides an alternative form for the unnormalized conditional state of Eq. (31) as

$$\rho_\pm = \frac{1}{2} (P_\pm^{\text{con}} \mathbf{I}_2 + \vec{r}_\pm \cdot \vec{\sigma}), \quad (34)$$

with the real vector

$$\vec{r}_\pm = \frac{1}{2} (A U_\xi + \vec{c}) \vec{r} \pm \sqrt{(1-p_c)p_c} (t_0^* \vec{t} + t_0 \vec{t}^* + i \vec{t} \times \vec{t}^* + A_t U_\xi \vec{r}). \quad (35)$$

After the measurement of the control qubit, the probe qubit terminates in the (normalized conditional) state

$$\rho_\pm^{\text{post}} = \frac{1}{P_\pm^{\text{con}}} \rho_\pm = \frac{1}{2} (\mathbf{I}_2 + \vec{r}_\pm^{\text{post}} \cdot \vec{\sigma}), \quad (36)$$

characterized by the post-measurement Bloch vector

$$\vec{r}_{\pm}^{\text{post}} = \frac{\vec{r}_{\pm}}{P_{\pm}^{\text{con}}}, \quad (37)$$

which is completely known via Eqs. (35) and (32).

An important observation is that, upon measuring the control qubit, the probabilities P_{\pm}^{con} of Eq. (32) governing the measurement outcomes, are in general influenced by the unitary U_{ξ} , via Q_{ξ} of Eq. (33). The control qubit and its measurement can therefore be exploited to extract information about U_{ξ} . It is the probe qubit that interacts with the unitary U_{ξ} , while the control qubit never directly interacts with U_{ξ} . Nevertheless, the dependence of P_{\pm}^{con} on U_{ξ} in Eq. (32) reveals that it is possible to measure the control qubit alone, while discarding the probe qubit, and obtain information about the unitary U_{ξ} . This possibility requires a genuine quantum superposition of two distinct channels in Fig. 1, since the dependence of P_{\pm}^{con} on U_{ξ} , as indicated by Eq. (32), vanishes for the control at $p_c = 0$ or 1 when no superposition exists.

A similar property of a control qubit dependent on U_{ξ} was also observed in [9] for a switched channel with indefinite causal order, although the study in [9] was restricted to a depolarizing noise $\mathcal{N}(\cdot)$ in Fig. 2 to enable an analytical characterization of the (more involved) switched channel. Here with the coherently superposed channel, the property of a U_{ξ} -dependent control qubit is generically established in broader conditions, for any qubit noise $\mathcal{N}(\cdot)$ in Fig. 2 and environment model. Although the mechanisms are different in the superposed channel here and in the switched channel of [9], both realize a coherent control of two channels resulting in a coupling of the probe and control qubits enabling a U_{ξ} -dependent control qubit that can be measured alone to extract information about U_{ξ} sensed by the probe qubit alone. This is a remarkable property, not found in conventional metrological techniques [14, 15, 16], where auxiliary inactive qubits that do not directly interact with the probed process usually need to be measured coherently with the active probing qubits in order to be of some use.

The general description we have obtained of the operation and measurement of the coherently superposed qubit channel, will now be applied to a task of phase estimation on the noisy qubit unitary U_{ξ} engaged in the coherent superposition.

6 Phase estimation from the superposed channel

So we now concentrate, as in [9], on the task of estimating the phase ξ of the unitary U_{ξ} . Phase estimation is an important task of quantum metrology, useful for instance in interferometry, magnetometry, frequency standards, atomic clocks, and many other high-precision high-sensitivity physical measurements [14, 15, 17, 18, 19, 20]. The axis \vec{n} of the qubit unitary U_{ξ} of Eq. (16) is assumed to be known, as fixed by the metrological setting, for instance as set by the orientation of the beam splitter of an interferometer, along with an unknown phase shift ξ between its two arms that is to be estimated. This is a common setting in metrology, where the phase ξ being estimated is intended to provide an image of a scalar physical quantity of metrological interest. A fundamental tool for assessing and comparing the efficiency of different strategies for parameter estimation is provided by the Fisher information, which we now consider.

6.1 Classical Fisher information for the control qubit

Statistical estimation theory [21, 22] stipulates that, from measured data dependent upon a parameter ξ , any conceivable estimator $\widehat{\xi}$ for ξ is endowed with a mean-squared error $\langle (\widehat{\xi} - \xi)^2 \rangle$ lower bounded

by the Cramér-Rao inequality, for unbiased as well as for biased estimators with an extended form of the inequality [23]. The lower bound to the mean-squared error involves the reciprocal of the classical Fisher information $F_c(\xi)$. The larger the Fisher information $F_c(\xi)$, the more efficient the estimation can be. The maximum-likelihood estimator [21, 22] is known to achieve the best efficiency dictated by the Cramér-Rao lower bound and Fisher information $F_c(\xi)$, at least in the asymptotic regime of a large number of independent data points. The classical Fisher information $F_c(\xi)$ stands in this respect as a fundamental metric quantifying the best achievable efficiency in estimation.

In the superposed channel, for estimating the phase ξ through the measurement of the control qubit displaying the two outcomes characterized by the probabilities P_+^{con} and $P_-^{\text{con}} = 1 - P_+^{\text{con}}$ of Eq. (32), the classical Fisher information [24] is

$$F_c^{\text{con}}(\xi) = \frac{(\partial_\xi P_+^{\text{con}})^2}{P_+^{\text{con}}} + \frac{(\partial_\xi P_-^{\text{con}})^2}{P_-^{\text{con}}} = \frac{(\partial_\xi P_+^{\text{con}})^2}{(1 - P_+^{\text{con}})P_+^{\text{con}}}. \quad (38)$$

From Eq. (32) we have the derivative

$$\partial_\xi P_+^{\text{con}} = \sqrt{(1 - p_c)p_c} \partial_\xi Q_\xi = \sqrt{(1 - p_c)p_c} \vec{s} \partial_\xi U_\xi \vec{r}. \quad (39)$$

The Fisher information $F_c^{\text{con}}(\xi)$ of Eq. (38) follows as

$$F_c^{\text{con}}(\xi) = \frac{4(1 - p_c)p_c(\partial_\xi Q_\xi)^2}{1 - 4(1 - p_c)p_c Q_\xi^2}. \quad (40)$$

The Fisher information $F_c^{\text{con}}(\xi)$ of Eq. (40) is maximized at $p_c = 1/2$, which amounts to preparing the control qubit in the state $|\psi_c\rangle = |+\rangle$ realizing an equiweighted superposition of the two elementary channels in Fig. 1; we shall stick to this favorable condition $p_c = 1/2$ in the sequel. The Fisher information of Eq. (40) then follows as

$$F_c^{\text{con}}(\xi) = \frac{(\partial_\xi Q_\xi)^2}{1 - Q_\xi^2} = \frac{(\vec{s} \partial_\xi U_\xi \vec{r})^2}{1 - (t_0 t_0^* + \vec{t} \vec{t}^* + \vec{s} U_\xi \vec{r})^2}. \quad (41)$$

For the rotated Bloch vector $\vec{r}_1(\xi) = U_\xi \vec{r}$, a geometric characterization of the derivative is provided in [24] as

$$\partial_\xi \vec{r}_1(\xi) = \partial_\xi U_\xi \vec{r} = \vec{n} \times \vec{r}_1(\xi). \quad (42)$$

The Fisher information of Eq. (41) then becomes

$$F_c^{\text{con}}(\xi) = \frac{[(\vec{s} \times \vec{n}) \cdot \vec{r}_1]^2}{1 - (t_0 t_0^* + \vec{t} \vec{t}^* + \vec{s} \cdot \vec{r}_1)^2}, \quad (43)$$

since $\vec{s}(\vec{n} \times \vec{r}_1) = (\vec{s} \times \vec{n}) \cdot \vec{r}_1$.

Then Eq. (43) shows that a favorable configuration to maximize the Fisher information $F_c^{\text{con}}(\xi)$ is to have an axis \vec{n} orthogonal to the vector \vec{s} of \mathbb{R}^3 so as to maximize the magnitude of $\vec{s} \times \vec{n}$, and in addition to prepare an input probe with unit Bloch vector \vec{r} also orthogonal to \vec{n} so that the rotated Bloch vector $\vec{r}_1(\xi) = U_\xi \vec{r}$ always remains in the plane orthogonal to \vec{n} for any angle ξ to estimate. Such an optimal configuration is achieved for instance with $\vec{n} \perp \vec{s}$ and $\vec{r} \parallel \vec{s}$, as depicted in Fig. 3.

The configuration of Fig. 3 yields in Eq. (43) the Fisher information

$$F_c^{\text{con}}(\xi) = \frac{\|\vec{s}\|^2 \sin^2(\xi)}{1 - [t_0 t_0^* + \vec{t} \vec{t}^* + \|\vec{s}\| |\cos(\xi)|]^2}. \quad (44)$$

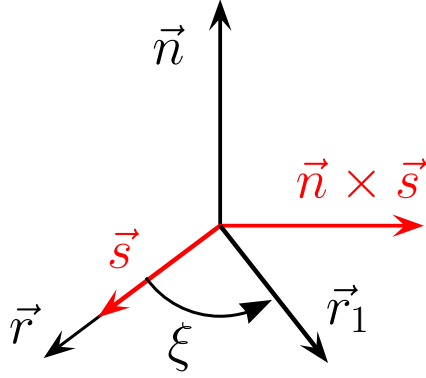


Figure 3: The vectors in \mathbb{R}^3 from the coherently superposed channel ensuring maximum estimation efficiency $F_c^{\text{con}}(\xi)$ in Eq. (43), with the rotation axis \vec{n} orthogonal to \vec{s} of Eq. (28), an input probe of unit Bloch vector $\vec{r} \parallel \vec{s}$, and a rotated Bloch vector $\vec{r}_1(\xi) = U_\xi \vec{r}$ remaining orthogonal to \vec{n} for any phase angle ξ to be estimated.

We know from Eqs. (22)–(23) and the example of the Pauli noises, that the real vector \vec{s} of Eq. (28) depends on both the noise parameters and the environment model via the products $\langle g|e_j\rangle$, and is independent of the unitary U_ξ under estimation. Therefore, for any conditions on the noise and environment model fixing \vec{s} , the arrangement of Fig. 3 will maximize the classical Fisher information at the level of Eq. (44), upon measuring the control qubit in the Fourier basis for estimating the phase ξ . The maximum Fisher information of Eq. (44) represents a useful reference. It will be achieved in practice if the unitary U_ξ can be operated with an axis $\vec{n} \perp \vec{s}$, for instance by properly orienting the interferometer. Otherwise, the efficiency $F_c^{\text{con}}(\xi)$ will be reduced according to the configuration of $\vec{s} \times \vec{n}$ as dictated by Eq. (43).

6.2 Quantum Fisher information for the control qubit

To complement the classical Fisher information, further assessment of the estimation performance can be obtained by means of the quantum Fisher information [25, 26]. For a ξ -dependent qubit state ρ_ξ of Bloch vector \vec{r}_ξ , the quantum Fisher information relative to the parameter ξ can be expressed [24] as

$$F_q(\xi) = \frac{(\vec{r}_\xi \partial_\xi \vec{r}_\xi)^2}{1 - \vec{r}_\xi^2} + (\partial_\xi \vec{r}_\xi)^2, \quad (45)$$

for the general case of a mixed state ρ_ξ , while it reduces to $F_q(\xi) = (\partial_\xi \vec{r}_\xi)^2$ for the special case of a pure state ρ_ξ . The usefulness of $F_q(\xi)$ is that it provides an upper bound to the classical Fisher information $F_c(\xi)$ attached to any quantum measurement protocol, by imposing $F_c(\xi) \leq F_q(\xi)$. There might not always exist a fixed ξ -independent measurement protocol to achieve $F_c(\xi) = F_q(\xi)$, however iterative strategies implementing adaptive measurements [25, 27, 28, 29, 30, 31, 32] are accessible to achieve $F_c(\xi) = F_q(\xi)$. The quantum Fisher information $F_q(\xi)$ is therefore a meaningful metric to characterize the overall best performance for quantum estimation.

When the control qubit is measured for estimating the phase ξ while the probe qubit is left untouched or unobserved, it is possible to assign a ξ -dependent state ρ_ξ^{con} to the control qubit by tracing over the probe qubit in the joint probe-control state $\mathcal{S}(\rho \otimes \rho_c)$ of Eq. (20), yielding

$$\begin{aligned} \rho_\xi^{\text{con}} = \text{tr}_{\text{probe}}[\mathcal{S}(\rho \otimes \rho_c)] &= \text{tr}[\mathcal{S}_{00}(\rho)] [p_c |0_c\rangle\langle 0_c| + (1 - p_c) |1_c\rangle\langle 1_c|] \\ &+ \text{tr}[\mathcal{S}_{01}(\rho)] \sqrt{(1 - p_c)p_c} (|0_c\rangle\langle 1_c| + |1_c\rangle\langle 0_c|). \end{aligned} \quad (46)$$

From Eq. (21) one has $\text{tr}[S_{00}(\rho)] = 1$, and $\text{tr}[S_{01}(\rho)] = Q_\xi$ of Eq. (33), so that one finally obtains

$$\rho_\xi^{\text{con}} = p_c |0_c\rangle\langle 0_c| + (1 - p_c) |1_c\rangle\langle 1_c| + \sqrt{(1 - p_c)p_c} Q_\xi (|0_c\rangle\langle 1_c| + |1_c\rangle\langle 0_c|), \quad (47)$$

which represents the qubit state characterized by the Bloch vector $\vec{r}_\xi^{\text{con}} = [2\sqrt{(1 - p_c)p_c}Q_\xi, 0, 2p_c - 1]^\top$. The measurement in the Fourier basis $\{|+\rangle, |-\rangle\}$ of the control qubit is equivalent to measuring the spin observable $\vec{\omega}_c \cdot \vec{\sigma}$ characterized in \mathbb{R}^3 by the vector $\vec{\omega}_c = \vec{e}_x = [1, 0, 0]^\top$. When acting on the qubit state ρ_ξ^{con} , this spin measurement leads to the two outcomes ± 1 with the probabilities

$$P_\pm^{\text{con}} = \frac{1}{2}(1 \pm \vec{\omega}_c \vec{r}_\xi^{\text{con}}) \quad (48)$$

coinciding with Eq. (32), while the classical Fisher information is

$$F_c^{\text{con}}(\xi) = \frac{(\vec{\omega}_c \partial_\xi \vec{r}_\xi^{\text{con}})^2}{1 - (\vec{\omega}_c \vec{r}_\xi^{\text{con}})^2} \quad (49)$$

coinciding with Eq. (38). With the derivative $\partial_\xi \vec{r}_\xi^{\text{con}} = [2\sqrt{(1 - p_c)p_c} \partial_\xi Q_\xi, 0, 0]^\top$, Eq. (45) provides the quantum Fisher information $F_q^{\text{con}}(\xi)$ associated with the control qubit as

$$F_q^{\text{con}}(\xi) = \frac{[4(1 - p_c)p_c Q_\xi \partial_\xi Q_\xi]^2}{4(1 - p_c)p_c(1 - Q_\xi^2)} + 4(1 - p_c)p_c (\partial_\xi Q_\xi)^2 \quad (50)$$

$$= 4(1 - p_c)p_c \frac{(\partial_\xi Q_\xi)^2}{1 - Q_\xi^2}, \quad (51)$$

forming an upper bound to $F_c^{\text{con}}(\xi)$ of Eq. (40) as it should. Just like the classical Fisher information $F_c^{\text{con}}(\xi)$ of Eq. (40), the quantum Fisher information $F_q^{\text{con}}(\xi)$ of Eq. (51) is maximized at $p_c = 1/2$, providing an additional motivation to this favorable configuration for preparing the control qubit. Then at $p_c = 1/2$, one has

$$F_q^{\text{con}}(\xi) = \frac{(\partial_\xi Q_\xi)^2}{1 - Q_\xi^2}, \quad (52)$$

which coincides with the classical Fisher information $F_c^{\text{con}}(\xi)$ of Eqs. (41) or (43). In this way, the choice $p_c = 1/2$ for the control qubit maximizes the quantum Fisher information $F_q^{\text{con}}(\xi)$, and in addition achieves $F_c^{\text{con}}(\xi) = F_q^{\text{con}}(\xi)$ for the measurement in the Fourier basis of the control qubit, for any \vec{s} and its configuration in relation to the axis \vec{n} and input probe \vec{r} . In other words, this indicates that there exists a fixed measurement protocol of the control qubit, the measurement in the Fourier basis or equivalently via the spin observable $\vec{\omega}_c \cdot \vec{\sigma}$ with $\vec{\omega}_c = \vec{e}_x$, able to reach $F_c^{\text{con}}(\xi) = F_q^{\text{con}}(\xi)$ — while as we indicated the existence of such an optimal measurement is not granted for all quantum estimation tasks. The choice $p_c = 1/2$ and the measurement in the Fourier basis for the control qubit, thus constitute the most efficient strategy for estimating the phase ξ from the control qubit of the superposed channel; and this is equally true for any noise $\mathcal{N}(\cdot)$ and environment model.

6.3 Coupling by the noise

The present analysis reveals the significant property that a non-vanishing noise $\mathcal{N}(\cdot)$ in Fig. 2 is necessary to couple the control qubit to the unitary U_ξ and enable estimation of the phase ξ from the control qubit of the superposed channel. A vanishing noise $\mathcal{N}(\cdot)$ in Fig. 2 is represented by one

trivial Kraus operator $\Lambda_1 = I_2$ while the other Λ_j are the null operator. This implies in the Bloch representation of Eq. (23) a single nonzero coordinate $t_0 = \langle g|e_1\rangle$ while $\vec{t} = \vec{0}$. In turn, $\vec{t} = \vec{0}$ implies $\vec{s} = \vec{0}$ in Eq. (28) and a factor Q_ξ in Eq. (33) becoming independent of the unitary U_ξ . As a result, the measurement probabilities P_\pm^{con} of Eq. (32) are independent of U_ξ . Follows also $\partial_\xi Q_\xi = 0$, so that the Fisher informations $F_c^{\text{con}}(\xi)$ in Eq. (40) and $F_q^{\text{con}}(\xi)$ in Eq. (51) both vanish, indicating that the control qubit is inoperative for estimating the phase ξ .

In addition, $\vec{t} = \vec{0}$ leads in Eq. (30) to $\mathcal{S}_{01}(\rho) = |t_0|^2(I_2 + U_\xi \vec{r} \cdot \vec{\sigma})/2 = |t_0|^2 U_\xi \rho U_\xi^\dagger$. The joint state of Eq. (20) factorizes as $\mathcal{S}(\rho \otimes \rho_c) = U_\xi \rho U_\xi^\dagger \otimes [p_c |0_c\rangle\langle 0_c| + (1 - p_c) |1_c\rangle\langle 1_c| + |t_0|^2 \sqrt{(1 - p_c)p_c}(|0_c\rangle\langle 1_c| + |1_c\rangle\langle 0_c|)]$ indicating that the probe and control qubits evolve separately, with a control qubit uncoupled to U_ξ . This shows that with no noise $\mathcal{N}(\cdot)$ in Fig. 2, although the state ρ_c of the control qubit is indeed affected, there is however no coupling of the control qubit to the unitary U_ξ which is seen only by the probe qubit. A non-vanishing noise is required to couple the control qubit to the unitary U_ξ , via its coupling with the probe qubit as described by Eq. (20) in the operation of the coherently superposed channel. And this is generically true for any type of noise and environment model.

This same property of noise-induced coupling was also observed in the switched channel with indefinite causal order studied in [9]. This property occurs in the presence of two distinguishable channels (1) and (2) superposed in Fig. 1 or switched in [9]. With no noise, the two channels (1) and (2) in Fig. 1 reduce to two identical and indistinguishable copies of the unitary U_ξ , so that the two paths driven by the control qubit are two indistinguishable paths offering limited versatility to the probe qubit. By contrast, in the presence of noise, the two channels (1) and (2) in Fig. 1 involve non-commuting Kraus operators, probabilistically combined, and occurring in two independent realizations; this results in two distinct paths driven by the control qubit, offering more versatility to the probe qubit, and realizing a quantum superposition of paths representing a specific nontrivial resource for information processing, as also argued in [3].

The noise $\mathcal{N}(\cdot)$ in the setting of Fig. 2, if it grows too large, may be expected also to arrive at some detrimental impact on the estimation performance. We may expect in this way an intermediate amount of noise able to maximize the estimation performance from the control qubit, that we will explicitly quantify in specific conditions in the sequel. Such a beneficial role of noise, here in the superposed channel or in the switched channel of [9], more broadly is reminiscent of an effect of stochastic resonance, which represents a general phenomenon occurring in various scenarios of information processing, classical [33, 34, 35, 36] or quantum [37, 38, 39, 40, 41], and where maximum efficiency is obtained at a nonzero optimal amount of noise.

We note also that the coupling of the control qubit to the unitary U_ξ , conveyed by the factor Q_ξ in Eq. (33) governing the Fisher informations $F_c^{\text{con}}(\xi)$ in Eq. (40) and $F_q^{\text{con}}(\xi)$ of Eq. (51), is essentially mediated by the vector \vec{s} of Eq. (28). This vector \vec{s} of Eq. (28) can especially survive (does not necessarily vanish) in configurations with small t_0 and large \vec{t} , as they would be achieved by noises with Kraus operators applying small probabilistic weight to the trivial operator I_2 , i.e. noises altering the qubit state with large probability. Such strong noise configurations, although presumably not optimal, may be expected to preserve some capability of the control qubit for phase estimation. In the sequel, in more definite conditions, we will further characterize this valuable property of the control qubit of the superposed channel, to preserve a capability for phase estimation in the presence of very large noise (when conventional estimation techniques fail, as we shall see).

6.4 Dependence on the noise implementation

As we have observed, the operation of the coherently superposed channel depends, not only on the Kraus operators describing each channel (1) and (2) in the superposition, but also on the Stinespring representation of each channel, specially via the initial state $|g\rangle$ of the environment model in the

implementation of each channel. This dependence is encapsulated in the two transformation operators T_1 and T_2 of Eqs. (8)–(9), acting in Eq. (13). This naturally has an impact when the coherently superposed channel analyzed in Section 2 is used for a task of phase estimation on the noisy qubit unitary of Fig. 2, as we address in the present Section 6. Phase estimation from the control qubit of the superposed channel is essentially governed by the two measurement probabilities P_{\pm}^{con} of Eq. (32). These probabilities P_{\pm}^{con} carry the dependence on the phase ξ via the real scalar factor Q_{ξ} of Eq. (33), which itself depends on the implementation of the noise $\mathcal{N}(\cdot)$ via the four Bloch coordinates (t_0, \vec{t}) of the operator T in Eq. (23). This implies that effective estimation of the phase ξ requires some knowledge of the parameters (t_0, \vec{t}) related to the noise implementation. When these parameters cannot be deduced from prior knowledge or assumptions available for the underlying environment, they represent unwanted unknown parameters; these are rather common in estimation theory and are commonly referred to as nuisance parameters [22, 21]. In practice, the presence of these nuisance parameters (t_0, \vec{t}) in the phase estimation task can be handled in different ways.

First, it can be noted that measurement of the control qubit, via its probabilities P_{\pm}^{con} of Eq. (32), gives direct access to an estimation of the scalar factor Q_{ξ} of Eq. (33). This factor Q_{ξ} then combines the effect of the unknown phase ξ of primary interest, and of the nuisance parameters (t_0, \vec{t}) . From an estimate of Q_{ξ} , the knowledge of (t_0, \vec{t}) is necessary if one wants to separate and deduce an estimate for the phase ξ . However, an estimate of Q_{ξ} alone may be sufficient in practice for some applications. A definite noise $\mathcal{N}(\cdot)$ in the setting of Fig. 2 is characterized by noise parameters (t_0, \vec{t}) that remain fixed while the phase ξ changes its value. This would be for instance the situation of an interferometer, with a definite noise $\mathcal{N}(\cdot)$ characterizing the interferometric setup, while operated for estimating the phase shift ξ occurring between its two arms, for metrological purposes. The standard modeling of a quantum noise $\mathcal{N}(\cdot)$ by means of a set of fixed Kraus operators, as given by Eq. (A-2), implies the presence of fixed environment parameters $(|g\rangle, |U_j\rangle)$ in the Stinespring implementation of a non-unitary channel. This is the same reason that induces fixed noise parameters (t_0, \vec{t}) for the operation of the coherently superposed channel. In a setup with fixed noise parameters (t_0, \vec{t}) , estimation of Q_{ξ} alone may be sufficient to track or distinguish different values of the phase ξ , which would not be known in their absolute physical values, but up to some fixed constants determined by (t_0, \vec{t}) as a characteristic of the metrological instrument. In the estimation of the scalar factor Q_{ξ} , the performance is governed by the classical Fisher information $F_c(Q_{\xi})$, which relates to the Fisher information $F_c(\xi)$ of Eqs. (38)–(40) for the phase ξ , by $F_c(\xi) = (\partial Q_{\xi}/\partial \xi)^2 F_c(Q_{\xi})$. In particular, $F_c(Q_{\xi})$ is maximized also at $p_c = 1/2$ to reach $F_c(Q_{\xi}) = 1/(1 - Q_{\xi}^2)$. In the same way for the quantum Fisher information, $F_q(\xi) = (\partial Q_{\xi}/\partial \xi)^2 F_q(Q_{\xi})$, and $F_q(Q_{\xi})$ is also maximized at $p_c = 1/2$ to reach $F_q(Q_{\xi}) = 1/(1 - Q_{\xi}^2)$, as compared to $F_q(\xi)$ of Eq. (52). The performance for estimating ξ or Q_{ξ} from the control qubit are therefore closely related; in particular the scheme operated at $p_c = 1/2$ and achieving $F_c(Q_{\xi}) = F_q(Q_{\xi})$ is also optimal for estimating Q_{ξ} . An additional interesting feature is that the Fisher informations involved (and involving Q_{ξ}^2) never vanish on average, when envisaged as averages over the phase ξ or over the noise parameters (t_0, \vec{t}) , indicating that the estimation capabilities of the control qubit are preserved in broad configurations of the parameters.

Second, a more thorough approach would be to envisage to estimate the value of the fixed nuisance parameters (t_0, \vec{t}) characterizing the estimation setup. This can be accomplished, as for the phase ξ , by measuring the control qubit alone in the coherently superposed channel. This would again deliver first, via the measurement probabilities P_{\pm}^{con} of Eq. (32), an estimate for the scalar factor Q_{ξ} of Eq. (33). A calibration procedure could then be envisaged, consisting, from estimates of Q_{ξ} obtained with known test values of the phase ξ arranged for calibration purposes, to deduce an estimate for (t_0, \vec{t}) . These fixed values estimated for the nuisance parameters (t_0, \vec{t}) would lead to a setup (an interferometer) fit for estimation of unknown phases ξ . More adequately, estimation is required (and performed from Q_{ξ} in the calibration) rather of the four real scalar parameters $s_0 = t_0 t_0^* + \vec{t} \vec{t}^*$

and $\vec{s} = [s_x, s_y, s_z]^T$ from Eq. (28), instead of the four scalar (t_0, \vec{t}) . An access to \vec{s} especially enables one to use the estimation setup in the optimal configuration characterized in Fig. 3, and (s_0, \vec{s}) also provide access to the Fisher informations relevant for performance assessment, so that with known (s_0, \vec{s}) then knowledge of (t_0, \vec{t}) is unnecessary. At this occasion we can stress this significant property of the coherently superposed channel. The operation of the coherently superposed channel is indeed dependent on the environment model implementing each of the non-unitary channels in the superposition. However, this dependence is encapsulated in a concise transformation operator as in Eqs. (8)–(9), which, when superposing two identical qubit channels, reduces to a qubit operator as \mathbb{T} in Eq. (23), characterizable with only four scalar parameters (t_0, \vec{t}) or (s_0, \vec{s}) . This is true independently of the size or dimensionality (possibly large) of the environment and of its constitutive details: only four scalar parameters need be estimated in the calibration procedure.

Alternatively, instead of a prior calibration procedure, direct estimation of the 1 + 4 unknown parameters ξ and (s_0, \vec{s}) can be envisaged also by measuring the control qubit alone of the superposed channel. The maximum-likelihood estimator [21, 22] mentioned at the beginning of Section 6.1, and matching the performance dictated by the Fisher information, typically operates from L independent measurements of the control qubit repeatedly prepared in the same conditions. The L measurements, individually governed by the probabilities P_{\pm}^{con} of Eq. (32), deliver L_+ outcomes projecting on $|+\rangle$ and $L - L_+$ on $|-\rangle$, with the integer $L_+ \in \{0, 1, \dots, L\}$. From the binomial probability distribution of the L outcomes follows the log-likelihood $\mathcal{L} = L_+ \log(P_+^{\text{con}}) + (L - L_+) \log(1 - P_+^{\text{con}})$. From the measured data $(L_+, L - L_+)$, the maximum-likelihood estimator for the multiparameter set (ξ, s_0, \vec{s}) follows as the solution to $\arg \max_{(\xi, s_0, \vec{s})} \mathcal{L}$; while in the presence of known (s_0, \vec{s}) through prior calibration, the maximum-likelihood estimator for the single phase parameter ξ is the solution to $\arg \max_{\xi} \mathcal{L}$. Such a direct estimation of a whole set (ξ, s_0, \vec{s}) of unknown parameters can also be realized recursively, in an adaptive manner, where especially the estimation of \vec{s} is progressively updated to bring the setup in the optimal configuration of Fig. 3 maximizing the performance. Such adaptive strategies have proven useful in other areas of quantum estimation and allow one to reach or to come close to optimality [25, 27, 28, 29, 30, 31, 32].

6.5 Analysis with Pauli noise

For further, more definite, illustration, we consider the interesting case already mentioned in Section 4 where $\mathcal{N}(\cdot)$ is a generic Pauli noise [12, 13] with the four Kraus operators $\{\Lambda_j\} = \{\sqrt{p_0}\mathbb{I}_2, \sqrt{p_x}\sigma_x, \sqrt{p_y}\sigma_y, \sqrt{p_z}\sigma_z\}$ and $\{p_j\}$ a probability distribution. For definiteness, we consider that the Pauli noise $\mathcal{N}(\cdot)$ is associated with an environment model starting in an unbiased initial state $|g\rangle$ satisfying $\langle g|e_j\rangle = 1/2$ for all $j = 1$ to 4. This represents an environment that does not specially favor any one of the underlying Kraus operators, but on the contrary that treats them in an even, equally weighted, manner. This is a reasonable configuration for an environment initially uncorrelated with the signal-control compound, realizing some kind of least biased or maximum entropy environment. This is also the choice that is considered for instance in the superposed channels investigated for information communication in [4, 7]. Such assumption on the noise constitution dispenses us from handling nuisance parameters as examined in Section 6.4. For the Bloch representation of \mathbb{T} in Eq. (23) we then have the coordinates $t_0 = \sqrt{p_0}/2$ and $\vec{t} = [\sqrt{p_x}, \sqrt{p_y}, \sqrt{p_z}]^T/2$, so that $t_0 t_0^* + \vec{t} \vec{t}^* = 1/4$, and $\vec{s} = 2t_0 \vec{t} = \sqrt{p_0}[\sqrt{p_x}, \sqrt{p_y}, \sqrt{p_z}]^T/2$ in Eq. (28) yielding $\|\vec{s}\|^2 = (1 - p_0)p_0/4$. The Fisher information from Eqs. (44) and (52) follows as

$$F_c^{\text{con}}(\xi) = F_q^{\text{con}}(\xi) = \frac{(1 - p_0)p_0 \sin^2(\xi)}{4 - \left[\frac{1}{2} + \sqrt{(1 - p_0)p_0} |\cos(\xi)|\right]^2}. \quad (53)$$

We observe that Eq. (53) now enables an explicit quantification of the intermediate amount of noise anticipated in Section 6.3 to maximize the performance of the control qubit. The estimation performance assessed by the Fisher information $F_c^{\text{con}}(\xi) = F_q^{\text{con}}(\xi)$ of Eq. (53) takes its maximum for a probability $p_0 = 1/2$, which is the situation where the noise maintains unaltered the qubit state (by applying the trivial Kraus operator $\Lambda_1 = \sqrt{p_0}I_2$) with probability 1/2. This behavior holds in the same way for any type of Pauli noise, irrespective of the other probabilities $\{p_x, p_y, p_z\}$ provided $p_x + p_y + p_z = 1 - p_0 = 1/2$. This remarkable property is obtained, from Eq. (43), with a rotation axis \vec{n} orthogonal to \vec{s} , with \vec{s} itself depending on $\{p_x, p_y, p_z\}$; otherwise, with \vec{n} and \vec{s} in another configuration, the value of $F_c^{\text{con}}(\xi) = F_q^{\text{con}}(\xi)$ given by Eq. (43) can be expected to be reduced relative to Eq. (53) and dependent on the noise probabilities $\{p_x, p_y, p_z\}$.

It can also be noted that the Fisher information $F_c^{\text{con}}(\xi) = F_q^{\text{con}}(\xi)$ of Eq. (53) bears an explicit dependence on the phase ξ , and this is also the rule in the more general conditions of Eqs. (44) or (43). This is a common property, often observed for quantum phase estimation in the presence of noise, and implying a performance varying according to the range of the phase ξ being estimated. A measurement result depending on ξ is necessary to enable estimation of ξ from such measurement. Commonly this entails also a measurement performance depending on ξ . For a performance assessment circumventing this dependence in ξ , it can be meaningful to consider the averaged Fisher information $\overline{F}_c = \int_0^{2\pi} F_c(\xi) d\xi / (2\pi)$ reflecting the average performance for values of the phase angle ξ uniformly covering the interval $[0, 2\pi)$. The averaged Fisher information \overline{F}_c also determines (via its reciprocal) a fundamental lower bound to the mean-squared estimation error in Bayesian estimation [21]. Here, for the Fisher information $F_c^{\text{con}}(\xi) = F_q^{\text{con}}(\xi)$ in Eq. (53) of the control qubit, the integral over ξ can be worked out explicitly to give

$$\overline{F}_c^{\text{con}}(\xi) = \overline{F}_q^{\text{con}}(\xi) = 1 - \frac{1}{2\pi} \left[\sqrt{9 - \beta^2} \arctan\left(\sqrt{\frac{3 + \beta}{3 - \beta}}\right) + \sqrt{25 - \beta^2} \arctan\left(\sqrt{\frac{5 - \beta}{5 + \beta}}\right) \right] \quad (54)$$

(where ξ is kept in the notation after the average to indicate the Fisher information is relative to the parameter ξ), with the noise factor

$$\beta = 2 \sqrt{(1 - p_0)p_0}. \quad (55)$$

And Eq. (54) will be useful for quantitative performance comparison to come.

7 Performance comparison

A meaningful reference for comparison is the Fisher information for estimating the phase ξ from a probing qubit that would directly interact with the noisy unitary channel of Fig. 2 in a single pass, with no coherent superposition of two copies of the channel. For the probing qubit prepared in the state ρ of Eq. (15), one pass through the channel of Fig. 2 is described by the quantum operation of Eq. (19), and it leaves the qubit in a state characterized by the Bloch vector

$$\vec{r}_\xi = AU_\xi \vec{r} + \vec{c} = A\vec{r}_1(\xi) + \vec{c}. \quad (56)$$

With the derivative $\partial_\xi \vec{r}_\xi = A\partial_\xi \vec{r}_1(\xi)$ characterized by Eq. (42), the quantum Fisher information is obtained from Eq. (45) as

$$F_q(\xi) = \frac{[(A\vec{r}_1 + \vec{c})A(\vec{n} \times \vec{r}_1)]^2}{1 - (A\vec{r}_1 + \vec{c})^2} + [A(\vec{n} \times \vec{r}_1)]^2. \quad (57)$$

When this standard probing qubit is measured, as the control qubit of the superposed channel by means of a spin observable $\vec{\omega} \cdot \vec{\sigma}$ characterized by a unit Bloch vector $\vec{\omega} \in \mathbb{R}^3$, the ensuing classical Fisher information is obtained from Eq. (49) as

$$F_c(\xi) = \frac{(\vec{\omega} \partial_\xi \vec{r}_\xi)^2}{1 - (\vec{\omega} \vec{r}_\xi)^2} = \frac{[\vec{\omega} A(\vec{n} \times \vec{r}_1)]^2}{1 - [\vec{\omega} (A\vec{r}_1 + \vec{c})]^2}. \quad (58)$$

It is then meaningful to compare the performance of such a standard probing qubit with the performance $F_c^{\text{con}}(\xi) = F_q^{\text{con}}(\xi)$ of Eq. (43) achieved at $p_c = 1/2$ by the control qubit of the coherently superposed channel measured in the Fourier basis with $\vec{\omega}_c = \vec{e}_x$.

For specifying the comparison in the conditions of Section 6.5, for the class of Pauli noises having $\vec{c} \equiv \vec{0}$, it is shown in [19] that a favorable configuration to maximize the quantum Fisher information $F_q(\xi)$ of Eq. (57) is when the rotated Bloch vector $\vec{r}_1(\xi)$ is a unit vector orthogonal to the rotation axis \vec{n} , which is obtained by a pure input probe with a unit Bloch vector \vec{r} also orthogonal to \vec{n} . This choice for the input probe maintains the rotated Bloch vector $\vec{r}_1(\xi)$ orthogonal to \vec{n} for any phase angle ξ . With \vec{r} and $\vec{r}_1(\xi)$ orthogonal to \vec{n} , there is however no fixed measurement vector $\vec{\omega}$ generally enabling the classical Fisher information $F_c(\xi)$ of Eq. (58) to reach the quantum Fisher information $F_q(\xi)$ of Eq. (57), even for a fixed type of Pauli noise. In general, achieving $F_c(\xi) = F_q(\xi)$ with the standard probing qubit, would require a vector $\vec{\omega}$ dependent on the noise matrix A but also on the unknown phase ξ under estimation, as it results from [19, 24]. By contrast, with the superposed channel, $F_c^{\text{con}}(\xi) = F_q^{\text{con}}(\xi)$ is achievable by $\vec{\omega}_c = \vec{e}_x$ for measuring the control qubit, uniformly for any noise and environment model, as we observed in Section 6.2.

For further quantitative comparison, it is interesting to work out the case of the qubit depolarizing noise, an important instance of Pauli noise [12, 13]. The depolarizing noise applies any one of the three non-trivial Pauli operators with equal probabilities $p_x = p_y = p_z = p/3$, while it leaves the qubit state ρ unchanged (or applies I_2) with the probability $p_0 = 1 - p$. In Eq. (18), along with $\vec{c} \equiv \vec{0}$, the resulting matrix A is the isotropic contraction matrix $A = \alpha I_3$ with $\alpha = 1 - 4p/3$ a scalar contraction factor, implementing an isotropic contraction of the qubit Bloch vector $\vec{r} \mapsto \alpha \vec{r}$. Equivalently, the action of the depolarizing noise can be described as

$$\mathcal{N}(\rho) = \alpha \rho + (1 - \alpha) \frac{I_2}{2}, \quad (59)$$

indicating that with the probability $1 - \alpha$, the noise replaces the qubit state ρ by the maximally mixed state $I_2/2$; at the maximum contraction when $\alpha = 0$, the quantum state is forced to $I_2/2$ with probability 1 and the qubit becomes completely depolarized. The depolarizing noise is an important noise model often considered in quantum information [12, 13]. It is a Pauli noise with no invariant subspace, unlike the bit-flip or phase-flip noises, and in this respect it represents in some sense a worse-case noise and as such a conservative reference.

With depolarizing noise, for the standard probing qubit, the quantum Fisher information of Eq. (57) becomes

$$F_q(\xi) = \alpha^2 (\vec{n} \times \vec{r}_1)^2 = \alpha^2 (\vec{n} \times \vec{r})^2, \quad (60)$$

and the classical Fisher information of Eq. (58),

$$F_c(\xi) = \frac{\alpha^2 [\vec{\omega} (\vec{n} \times \vec{r}_1)]^2}{1 - \alpha^2 (\vec{\omega} \vec{r}_1)^2}. \quad (61)$$

In the favorable configuration where \vec{r} and $\vec{r}_1(\xi)$ are in the plane orthogonal to the rotation axis \vec{n} , the quantum Fisher information of Eq. (60) is maximized at $F_q^{\text{max}}(\xi) = \alpha^2$ for any phase angle ξ . However,

as indicated, there is no fixed measurement vector $\vec{\omega}$ enabling $F_c(\xi)$ of Eq. (61) to reach $F_q^{\max}(\xi) = \alpha^2$, for any phase ξ . This would require an $\vec{\omega}$ orthogonal to the rotated Bloch vector $\vec{r}_1(\xi)$ for any ξ , which is not realizable since ξ is unknown. Alternatively, one can select $\vec{\omega}$ to coincide with the pure input probe \vec{r} , so that at $\vec{\omega} = \vec{r} \perp \vec{n}$, the classical Fisher information of Eq. (61) becomes

$$F_c(\xi) = \frac{\alpha^2 \sin^2(\xi)}{1 - \alpha^2 \cos^2(\xi)} \leq F_q(\xi) = \alpha^2. \quad (62)$$

This $F_c(\xi)$ is to be compared with $F_c^{\text{con}}(\xi) = F_q^{\text{con}}(\xi)$ of Eq. (53) with for the depolarizing noise the factor $(1 - p_0)p_0 = 3(1 + 3\alpha)(1 - \alpha)/16$, or the equivalent form of Eq. (53) as

$$F_c^{\text{con}}(\xi) = F_q^{\text{con}}(\xi) = \frac{\beta^2 \sin^2(\xi)}{16 - [1 + \beta |\cos(\xi)|]^2}, \quad (63)$$

with the factor β of Eq. (55) expressed as a function of the contraction factor α as

$$\beta = \frac{\sqrt{3}}{2} \sqrt{(1 - \alpha)(1 + 3\alpha)}. \quad (64)$$

The performance of Eq. (63) is achieved in the superposed channel by the control qubit in the optimal configuration of Fig. 3 with a vector \vec{s} in Eq. (28) which for the depolarizing noise is $\vec{s} = \beta/(4\sqrt{3})[1, 1, 1]^\top = \beta/(4\sqrt{3})\vec{1}$. This is obtained with an axis $\vec{n} \perp \vec{1}$ and an input probe $\vec{r} \parallel \vec{1}$, uniformly for any level α of the depolarizing noise. By contrast, as we indicated, the standard probing qubit in general cannot reach $F_c(\xi) = F_q(\xi)$ in Eq. (62) or (61).

Then the Fisher informations of Eqs. (62) and (63) offer a meaningful basis for quantitative comparison. It can be noted that all of them depend on the value of the phase ξ under estimation. As indicated at the occasion of Eq. (53), to circumvent the ξ -dependent performance it is convenient to consider the phase-averaged Fisher information for a phase ξ uniformly covering the interval $[0, 2\pi)$. For the control qubit of the coherently superposed channel, such phase averaging of Eq. (63) leads to $\overline{F}_c^{\text{con}}(\xi) = \overline{F}_q^{\text{con}}(\xi)$ of Eq. (54) with β from Eq. (64). Meanwhile, for the standard probing qubit the phase averaging of Eq. (62) yields

$$\overline{F}_c(\xi) = 1 - \sqrt{1 - \alpha^2} \leq \overline{F}_q(\xi) = \alpha^2. \quad (65)$$

For comparison, we also consider the phase-averaged Fisher information achieved by the control qubit of a switched channel with indefinite causal order, as analyzed in [9], which is given by

$$\overline{F}_c^{\text{swi}}(\xi) = \overline{F}_q^{\text{swi}}(\xi) = 1 - \frac{\sqrt{3}}{8}(1 - \alpha) \sqrt{(1 - \alpha)(3 + 5\alpha)} - \frac{1}{8} \sqrt{(5 + 6\alpha - 3\alpha^2)(5 - 2\alpha + 5\alpha^2)}, \quad (66)$$

reproducing Eq. (44) of [9].

The three phase-averaged Fisher informations are compared in Fig. 4, as a function of the level of the depolarizing noise quantified by its contraction factor α .

As visible in Fig. 4, for most noise levels α , the straightforward approach of the standard probing qubit is more efficient, with a larger Fisher information $\overline{F}_c(\xi)$. At vanishing noise, when $\alpha \rightarrow 1$, the Fisher information $\overline{F}_c(\xi)$ of Eq. (65) goes to 1 and reaches its upper bound $\overline{F}_q(\xi) = \alpha^2 \rightarrow 1$ where the estimation efficiency of the standard probing qubit is maximal. By contrast, the control qubit of the superposed channel, at vanishing noise when $\alpha \rightarrow 1$, as anticipated in Section 6.3, becomes inoperative for estimating the phase ξ , as marked by a vanishing Fisher information $\overline{F}_c^{\text{con}}(\xi) = \overline{F}_q^{\text{con}}(\xi)$ in Fig. 4. In addition, Fig. 4 also shows the existence of an optimal level of noise where the efficiency

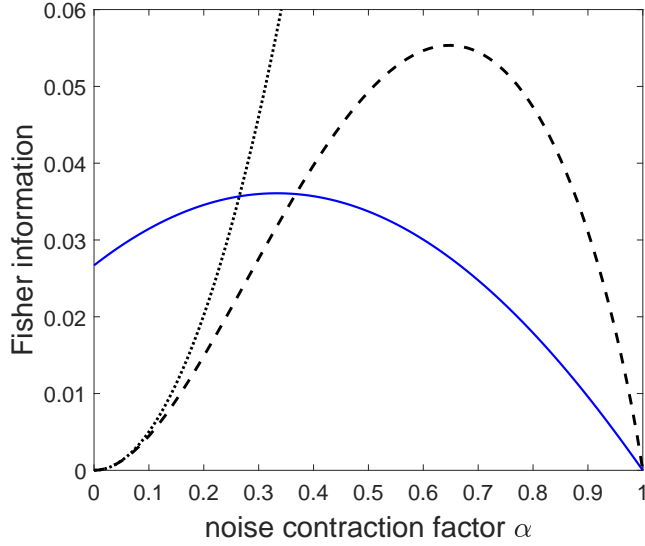


Figure 4: Phase-averaged Fisher information $\overline{F}_c^{\text{con}}(\xi) = \overline{F}_q^{\text{con}}(\xi)$ of Eq. (54) via Eq. (64) for the control qubit of the coherently superposed channel (solid line), $\overline{F}_c(\xi)$ of Eq. (65) for the standard probing qubit (dotted line), and $\overline{F}_c^{\text{swi}}(\xi) = \overline{F}_q^{\text{swi}}(\xi)$ of Eq. (66) for the control qubit of the switched channel with indefinite order of [9] (dashed line), as a function of the contraction factor α of the depolarizing noise of Eq. (59).

of the control qubit of the superposed channel is maximized, as also anticipated in Section 6.3. This is marked in Fig. 4 by a Fisher information $\overline{F}_c^{\text{con}}(\xi) = \overline{F}_q^{\text{con}}(\xi)$ culminating at a maximum for $\alpha \approx 0.34$.

An interesting feature shown in Fig. 4 is that when the noise becomes fully depolarizing, at $\alpha \rightarrow 0$, the Fisher information $\overline{F}_c^{\text{con}}(\xi) = \overline{F}_q^{\text{con}}(\xi)$ of the control qubit of the superposed channel does not go to zero, while $\overline{F}_c(\xi)$ and $\overline{F}_q(\xi)$ vanish for the standard probing qubit. At $\alpha \rightarrow 0$, the standard probing qubit ruled by Eq. (19) with $A = \alpha I_3$ and $\vec{c} \equiv \vec{0}$, experiences the input–output transformation $\rho \mapsto I_2/2$, producing a completely depolarized output state $I_2/2$ insensitive to the phase ξ , and therefore inoperative for its estimation, as expressed by the vanishing Fisher informations $\overline{F}_c(\xi)$ and $\overline{F}_q(\xi)$ in Eq. (65) and visible in Fig. 4. By contrast, via the coupling interaction taking place in the coherently superposed channel, the output state ρ_ξ^{con} of Eq. (47) for the control qubit remains sensitive to the phase ξ , even at $\alpha \rightarrow 0$, as expressed by the non-vanishing Fisher information $\overline{F}_c^{\text{con}}(\xi) = \overline{F}_q^{\text{con}}(\xi)$ in Fig. 4. This is a significant difference, with a fully depolarizing noise in the noisy unitary channel of Fig. 2, the standard probing qubit is unable to deliver information about the phase ξ ; by contrast, the control qubit of the superposed channel of Fig. 1, through the more elaborate coupling interaction analyzed here, remains operative for estimating ξ . This is a manifestation of the beneficial role of the noise in coupling the control qubit to the unitary U_ξ in the superposed channel, as discussed in Section 6.3. Accordingly, at strong noise, when the contraction factor $\alpha \lesssim 0.26$ in Fig. 4, the Fisher information, and therefore the efficiency for phase estimation, of the control qubit of the superposed channel, remain superior to those of the standard probing qubit.

In addition, the comparison with the switched channel with indefinite order of [9] shows in Fig. 4 a switched channel with a Fisher information $\overline{F}_c^{\text{swi}}(\xi) = \overline{F}_q^{\text{swi}}(\xi)$ of Eq. (66) also undergoing a non-monotonic evolution, as $\overline{F}_c^{\text{con}}(\xi) = \overline{F}_q^{\text{con}}(\xi)$ of Eq. (54) for the superposed channel, yet culminating at a maximum for a different noise level $\alpha \approx 0.65$. Also, for the noise contraction factor above the crossover $\alpha \approx 0.37$, the performance of the switched channel remains larger than that of the superposed channel. The operating mechanisms of the two channels are significantly different, but the larger performance can be related to the fact that the elementary path in the switched channel of [9]

includes two passes across the sensed unitary U_ξ , when the superposed channel here, in comparison, includes only one. A significant observation is that, at large noise when $\alpha \rightarrow 0$, the switched channel also exhibits a vanishing performance $\overline{F}_c^{\text{swi}}(\xi) = \overline{F}_q^{\text{swi}}(\xi) \rightarrow 0$, and becomes inoperative for phase estimation, just like the standard probing qubit; while, as we already mentioned, the superposed channel remains operative for estimation in this large-noise limit. This is a remarkable benefit observed with the coherently superposed channel, to maintain the possibility of phase estimation, even when the unitary U_ξ in Fig. 2 is buried in a fully depolarizing noise. No other estimation techniques are known to share this ability.

Another important difference is that the coherently superposed channel here, in order for its control qubit to reach the optimized performance of Eq. (44) or (54), requires a pure input probe with a unit Bloch vector \vec{r} prepared in the configuration of Fig. 3. By contrast, the switched channel of [9] exhibits a control qubit reaching the performance conveyed by Eq. (66) independently of the preparation \vec{r} of the input probe qubit. Especially, even when $\vec{r} = \vec{0}$ with a completely depolarized input probe qubit, the control qubit of the switched channel in [9] maintains its capability for phase estimation, with the performance of Eq. (66), but this capability disappears in the presence of a fully depolarizing noise $\mathcal{N}(\cdot)$ in Fig. 2. So the superposed channel here requires a pure input probe qubit optimized as in Fig. 3, but its capability for phase estimation persists even with a fully depolarizing noise $\mathcal{N}(\cdot)$; by contrast, the switched channel of [9] remains operative for phase estimation even with a completely depolarized input probe qubit, but its capability vanishes with a fully depolarizing noise $\mathcal{N}(\cdot)$. These are two distinct properties, stemming from the different mechanisms ruling the superposed or the switched channels, but that are not accessible with conventional estimation techniques. These unconventional properties can be related to the results in quantum communication of [3, 7, 4], also concerning completely depolarizing channels, which recover ability for information communication when they are combined into a switched channel with indefinite order in [3, 7] or into a coherently superposed channel in [4, 7]. Beyond quantum communication in [3, 7, 4], the possibility of recovering from fully depolarizing conditions, through coherent control on quantum channels, under different forms here and in [9], is extended to the fundamental metrological task of quantum phase estimation.

To further appreciate the beneficial role of noise in the operation of the coherently superposed channel, we can evaluate, as in [7], an index of non-commutativity χ_{NC} of the underlying Kraus operators, by means of a cumulated trace distance between their pairwise commutators, and defined in the conditions of Section 4 as $\chi_{\text{NC}} = \sum_{j,k} \text{tr}([K_j, K_k]^\dagger [K_j, K_k])$. In general this non-commutativity index χ_{NC} can be expected to depend on the parameters of the underlying Kraus operators, in particular here with the channels of Fig. 2 on the parameters of the unitary U_ξ and the noise $\mathcal{N}(\cdot)$. For illustration, for the channels with depolarizing noise studied in Section 7 and Fig. 4, the non-commutativity index evaluates to

$$\chi_{\text{NC}} = 8(1 - \alpha)\alpha \sin^2(\xi/2) + 3(1 - \alpha)^2, \quad (67)$$

which indeed depends on the unitary U_ξ via its phase ξ and on the noise via its contraction factor α . We observe, consistently, that the non-commutativity index χ_{NC} of Eq. (67) vanishes at $\alpha = 1$ when there is no noise and the Kraus operators commute. On the contrary, χ_{NC} in Eq. (67) tends to be large at strong noise when $\alpha \rightarrow 0$, showing that the noise is an essential ingredient to make the Kraus operators non-commuting and favor the probe-control coupling in the superposed channel, as discussed in Section 6.3. The phase-averaged index $\overline{\chi}_{\text{NC}} = 4(1 - \alpha)\alpha + 3(1 - \alpha)^2 = (1 - \alpha)(3 + \alpha)$ culminates at $\overline{\chi}_{\text{NC}} = 3$ at maximum noise when $\alpha = 0$ and monotonically decays to zero as $\alpha \rightarrow 1$. In these conditions, maximum noise achieves maximum non-commutativity of the Kraus operators. However, as discussed in Section 6.3, stronger noise, which favors non-commutativity and coupling, at some point arrives at a detrimental impact on the phase estimation efficiency, whence the intermediate level of noise as a compromise to maximize the performance of phase estimation from

the control qubit in the superposed channel, as reflected for instance in Fig. 4.

A non-vanishing Fisher information $F_c^{\text{con}}(\xi) = F_q^{\text{con}}(\xi)$ observed for the control qubit of the superposed channel in the presence of a fully depolarizing noise at $\alpha = 0$, is generically preserved with any underlying environment model. Instead of the unbiased environment characterized by $\langle g|e_j\rangle = 1/2$ for $j = 1$ to 4 chosen in Section 6.5, an arbitrary environment underlying the depolarizing noise of Eq. (59) can be handled with in Eq. (23) the general coordinates $t_0 = \langle g|e_1\rangle \sqrt{p_0} = \langle g|e_1\rangle \sqrt{1 + 3\alpha}/2$ and $\vec{t} = \vec{e} \sqrt{(1 - p_0)/3} = \vec{e} \sqrt{1 - \alpha}/2$ with the vector $\vec{e} = [\langle g|e_2\rangle, \langle g|e_3\rangle, \langle g|e_4\rangle]^\top$. As a result, for the vector \vec{s} of Eq. (28), we have $t_0^* \vec{t} = \langle g|e_1\rangle^* \vec{e} \sqrt{(1 + 3\alpha)(1 - \alpha)}/4$ and $\vec{t}^* \times \vec{t} = \vec{e}^* \times \vec{e} (1 - \alpha)/4$. As expressed by Eqs. (32)–(33), the vector \vec{s} , via the factor Q_ξ , carries the coupling of the control qubit to the unitary U_ξ , and therefrom the capability of the control qubit for phase estimation on U_ξ . The important property here is that \vec{s} vanishes, generically, with vanishing depolarizing noise at $\alpha = 1$ where $\vec{t} = \vec{0}$, as discussed in Section 6.3; but on the contrary \vec{s} does not vanish, generically, at maximum depolarizing noise when $\alpha = 0$ where $\vec{t} \neq \vec{0}$. In this way, with a fully depolarizing noise at $\alpha = 0$, the capability for phase estimation of the controlled qubit of the superposed channel is generically preserved, for any environment model implementing the depolarizing noise.

For further comparison, it can be considered that the superposed channel, with a control qubit and a probe qubit, is a two-qubit process, even when measuring only the control qubit for phase estimation. Accordingly, a comparison is meaningful also with two-qubit conventional schemes for estimation [14, 15, 16]. With two independent probing qubits, the performance of conventional schemes assessed by the Fisher information is additive, and is easily obtained from the characterization we performed above via Eqs. (57)–(58). With two entangled probing qubits, the performance of conventional schemes assessed by the Fisher information can be super-additive, benefiting from Heisenberg enhancement, which is nevertheless very fragile in the presence of noise [15, 16, 42]. But in any case, in the presence of a fully depolarizing noise $\mathcal{N}(\cdot)$, a standard interaction of the noisy unitary of Fig. 2 with a probing qubit, always outputs the completely depolarized state $I_2/2$ where any information about the unitary U_ξ is suppressed. Therefore, with two or even more independent or entangled probing qubits, conventional techniques will remain inoperative for phase estimation in the presence of fully depolarizing noise, while the control qubit of the superposed channel remains operative, as we have shown above.

In the coherently superposed channel, after measurement of the control qubit, the probe qubit gets placed in the conditional state ρ_\pm^{post} of Eqs. (36)–(37), which generally depends on the phase ξ , as expected for a qubit directly interacting with the unitary U_ξ . Measuring ρ_\pm^{post} can therefore provide additional information to estimate ξ . The performance upon measuring ρ_\pm^{post} is however more complicated to analyze and optimize, depending on the geometry as in Fig. 3, and the optimality conditions usually depend on which of the two conditional states ρ_+^{post} or ρ_-^{post} is obtained. An interesting property is that, with a fully depolarizing noise, the conditional Bloch vector $\vec{r}_\pm^{\text{post}}$ of Eq. (37) remains dependent on the phase ξ , and can therefore be exploited for its estimation, although it is to more difficult to do it optimally.

Finally, if one resorts to measuring the probe qubit as well as the control qubit, a joint measurement of the two-qubit state $\mathcal{S}(\rho \otimes \rho_c)$ of Eq. (20) could be envisaged as an alternative for estimation. This is a fortiori a more complicated strategy, to analyze, to optimize and to implement. Interesting properties could nevertheless result, based on the capabilities revealed by the analysis of the control qubit of the superposed channel we performed here.

8 Conclusion

We have analyzed the coherently superposed channel of Fig. 1 when superposing two copies of a qubit unitary operator U_ξ affected by a general qubit noise as in Fig. 2. A characterization has been developed for the joint state $\mathcal{S}(\rho \otimes \rho_c)$ in Eq. (20) of the probe-control qubit pair of the coherently superposed channel. As an application, an analysis of the superposed channel and its performance has been performed for the fundamental metrological task of phase estimation on the unitary U_ξ in the presence of noise. A comparison has also been made with conventional techniques of estimation and with the switched quantum channel with indefinite causal order studied in [9] for a similar task of phase estimation. In particular, the present study complements the recent study of [9], so as to obtain a consistent analysis of the capabilities of coherently controlled channels, superposed or switched, for the fundamental metrological task of quantum phase estimation on a noisy unitary operator.

A first important observation here is that the control qubit of the superposed channel, although it never directly interacts with the unitary U_ξ , can nevertheless be measured alone for effective estimation on U_ξ , while discarding the probe qubit that interacts with the unitary U_ξ . This property also occurs in the switched channel of [9], but it never occurs with conventional techniques where auxiliary inactive qubits must be measured with the active probing qubits to be of some use for estimation. This property of a U_ξ -dependent control qubit in the superposed channel, is generically established in broad conditions here, for any qubit noise $\mathcal{N}(\cdot)$ in Fig. 2 and underlying environment model. In addition, the optimal measurement of the control qubit with maximum efficiency for phase estimation, has been characterized in general conditions on the noise and environment.

A second important observation is that the noise plays an essential role in coupling the control qubit to the unitary U_ξ , with usually a nonzero amount of noise maximizing the efficiency of the control qubit for phase estimation on U_ξ . This is also established to hold generically in the superposed channel, for any qubit noise and environment model. In addition, it is observed that the control qubit of the superposed channel remains operative for phase estimation at very strong noise, even with a fully depolarizing noise with any implementing environment, whereas conventional estimation techniques and the switched channel with indefinite order of [9] become inoperative in these conditions. This represents here a specificity of the superposed channel that is significant for noisy quantum metrology. The fully depolarizing noise, which does not suppress the estimation capability in the superposed channel here, is reminiscent of the completely depolarizing channel that enables information communication when placed in coherently controlled associations, switched or superposed, as shown in [3, 7, 4]. However, the tasks and performance metrics are different for estimation and communication, and the present results provide additional elements for broader appreciation of the capabilities and specificities of coherently controlled channels — switched as well as superposed — as novel devices exploitable for various tasks of quantum information processing.

The characterization of the joint probe-control state $\mathcal{S}(\rho \otimes \rho_c)$ carried out in Section 4 could be further exploited for other purposes involving the noisy unitary placed in a coherent superposition. Estimation of the axis \vec{n} of the unitary could as well be envisaged, and due to the fundamental coupling described by Eqs. (32)–(33) via the U_ξ -dependent factor Q_ξ , such estimation again would be possible by measuring the control qubit alone.

As we have seen in the analysis, the operation of the coherently superposed channel and the joint probe-control state $\mathcal{S}(\rho \otimes \rho_c)$ of Eq. (10) it outputs, depend on the underlying implementation of the non-unitary channels realized by the environment. When superposing two identical qubit channels, as done for phase estimation on U_ξ , this dependence can be encapsulated in four real scalar parameters (s_0, \vec{s}) , independently of the size and constitutive details of the environment. If these parameters (s_0, \vec{s}) cannot be deduced from prior knowledge or assumptions available for the underlying environment, they can be included in the estimation process analyzed in the study and can be estimated from

measurement of the control qubit of the superposed channel. Such an estimation process of a few scalar parameters for the environment in fact provides a handle enabling to put in practical use coherently superposed qubit channels, for phase estimation as addressed here, but also for information communication as addressed in [4, 7], or for other tasks of quantum signal and information processing. For instance, in practice, based on the present analysis, a unitary process invincibly hidden in a fully depolarizing noise, could become amenable to estimation via its duplication and insertion in a interferometric setup as in [10, 11, 4] experimentally realizing the controlled coherent superposition. Other possibilities are opened for exploration by exploiting coherently controlled channels for quantum signal and information processing.

Appendix

In this Appendix we provide additional elements on the Stinespring implementation of quantum channels, like channels (1) and (2) of Section 2, and having special relevance for their coherent superposition as in Fig. 1. On a quantum system Q with Hilbert space \mathcal{H} , a quantum operation or channel $\rho \mapsto \mathcal{E}(\rho)$ defined by a set of K Kraus operators $\{K_j\}_{j=1}^K$ of $\mathcal{L}(\mathcal{H})$, can be obtained [12, 13] from an environment model E with a K -dimensional Hilbert space \mathcal{H}_E implementing on the joint system-environment compound QE the (dilated) unitary evolution

$$|\psi\rangle \otimes |g\rangle \xrightarrow{U_J} U_J |\psi\rangle \otimes |g\rangle = |\phi_{QE}\rangle \in \mathcal{H} \otimes \mathcal{H}_E, \quad (\text{A-1})$$

for any state $|\psi\rangle \in \mathcal{H}$ of system Q and where $|g\rangle \in \mathcal{H}_E$ is the initial state of the environment E . An orthonormal basis $\{|e_j\rangle\}_{j=1}^K$ of the K -dimensional environment space \mathcal{H}_E is used for performing partial tracing over the environment, in order to obtain the quantum operation on system Q as $\rho = |\psi\rangle\langle\psi| \mapsto \mathcal{E}(\rho) = \text{tr}_E(|\phi_{QE}\rangle\langle\phi_{QE}|) = \sum_{j=1}^K \langle e_j|\phi_{QE}\rangle\langle\phi_{QE}|e_j\rangle$. From Eq. (A-1) we obtain in this way the operator-sum representation of the quantum operation as $\mathcal{E}(\rho) = \sum_{j=1}^K K_j |\psi\rangle\langle\psi| K_j^\dagger$, defining the Kraus operators

$$K_j = \langle e_j|U_J|g\rangle, \quad (\text{A-2})$$

for $j = 1$ to K , via the notion of partial inner product [43, 12]. By linearity, the same operator-sum representation of $\mathcal{E}(\rho)$ applies when ρ is a mixed state as a convex sum of pure states like $|\psi\rangle\langle\psi|$. Then Eq. (A-2) enables us to write an equivalent form for the joint unitary evolution U_J of the system-environment compound QE of Eq. (A-1) as

$$|\psi\rangle \otimes |g\rangle \xrightarrow{U_J} \sum_{j=1}^K K_j |\psi\rangle \otimes |e_j\rangle = |\phi_{QE}\rangle \in \mathcal{H} \otimes \mathcal{H}_E, \quad (\text{A-3})$$

forming the ground for the evolutions of Eqs. (1)–(2). For a given quantum operation $\mathcal{E}(\cdot)$, the minimal number of Kraus operators is determined by the rank of $\mathcal{E}(\cdot)$ and is no larger than $[\dim(\mathcal{H})]^2$. Any two sets $\{K_j\}_{j=1}^K$ and $\{K'_k\}_{k=1}^{K'}$ of Kraus operators offer an equivalent operator-sum representation of the same quantum operation $\mathcal{E}(\cdot)$, if and only if they can be connected [12] via a unitary transformation

$$K'_k = \sum_{j=1}^{K'} u_{kj} K_j, \quad (\text{A-4})$$

where the smaller set of the two has been complemented with null operators to equalize the sizes K and K' , and the complex numbers $[u_{kj}]$ form a (square) unitary matrix, in particular satisfying $\sum_\ell u_{\ell j} u_{\ell k}^* = \delta_{jk}$ and $\sum_\ell u_{j\ell} u_{k\ell}^* = \delta_{jk}$, so that Eq. (A-4) inverts as $K_j = \sum_k u_{kj}^* K'_k$.

A given environment model fixed by $(|g\rangle, U_J)$ in Eq. (A-1), with dimension K , generates the set $\{K_j\}_{j=1}^K$ of K Kraus operators via Eq. (A-2) when the K -dimensional environment space \mathcal{H}_E is referred to the orthonormal basis $\{|e_j\rangle\}_{j=1}^K$. From here, a larger set $\{K'_k\}_{k=1}^{K'}$ of $K' \geq K$ Kraus operators offering an equivalent representation for the same quantum operation $\mathcal{E}(\cdot)$, can be obtained via Eq. (A-4), for any size $K' \geq K$, by fixing a unitary matrix $[u_{kj}]$. This larger set $\{K'_k\}_{k=1}^{K'}$ of $K' \geq K$ Kraus operators can be associated with an environment model E' , which, according to the logic above, will be tied to a larger Hilbert space \mathcal{H}'_E with dimension $K' \geq K$. This Hilbert space \mathcal{H}'_E can be selected in such a way that \mathcal{H}_E with dimension K for the environment E , is a subspace of \mathcal{H}'_E with dimension $K' \geq K$ for the environment E' , this corresponding to enlarging the number of degrees of freedom of the environment coupled to system Q .

From the unitary connection of Eq. (A-4), the set $\{K'_k\}_{k=1}^{K'}$ is recovered by the partial products $K'_k = \langle e'_k | U'_J | g \rangle$ by referring to the orthonormal basis $\{|e'_k\rangle\}_{k=1}^{K'}$ of \mathcal{H}'_E . This basis $\{|e'_k\rangle\}_{k=1}^{K'}$ of \mathcal{H}'_E is connected to the basis $\{|e_j\rangle\}_{j=1}^K$ of \mathcal{H}_E via the unitary transformation

$$|e'_k\rangle = \sum_{j=1}^{K'} u_{kj}^* |e_j\rangle \iff |e_j\rangle = \sum_{k=1}^{K'} u_{kj} |e'_k\rangle, \quad (\text{A-5})$$

where the smaller basis $\{|e_j\rangle\}_{j=1}^K$ of $\mathcal{H}_E \subseteq \mathcal{H}'_E$ has been complemented (in a non-critical way) by $K' - K$ orthonormal states $\{|e_j\rangle\}_{j=K+1}^{K'}$ to reach an orthonormal basis of \mathcal{H}'_E . In a comparable way, the unitary U'_J acting in the larger space $\mathcal{H} \otimes \mathcal{H}'_E$, has an action coinciding with U_J in $\mathcal{H} \otimes \mathcal{H}_E$, and is complemented outside in a non-critical way. The initial state $|g\rangle \in \mathcal{H}_E \subseteq \mathcal{H}'_E$ does not change while enlarging the environment dimensionality, and the evolution of the system-environment compound of Eq. (A-3) can be written in the two alternative forms

$$|\psi\rangle \otimes |g\rangle \mapsto \sum_{j=1}^K K_j |\psi\rangle \otimes |e_j\rangle = \sum_{k=1}^{K'} K'_k |\psi\rangle \otimes |e'_k\rangle = |\phi_{QE}\rangle \in \mathcal{H} \otimes \mathcal{H}_E \subseteq \mathcal{H} \otimes \mathcal{H}'_E. \quad (\text{A-6})$$

In this way, starting from a set $\{K_j\}_{j=1}^K$ of K Kraus operators and its generative environment model, we can deduce, by introducing an arbitrary unitary matrix $[u_{kj}]$, an infinite number of equivalent Kraus sets $\{K'_k\}_{k=1}^{K'}$ along with their generative environment model, and representing the same quantum operation $\mathcal{E}(\cdot)$. The significant feature for the superposed channel of Fig. 1 is that all these equivalent representations share the same transformation operators like T_1 and T_2 of Eqs. (8)–(9), since by the unitary connections of Eqs. (A-4)–(A-5) we generically have

$$T_1 = \sum_{j=1}^K \langle g | e_j \rangle K_j = \sum_{k=1}^{K'} \langle g | e'_k \rangle K'_k. \quad (\text{A-7})$$

Moreover, by expressing in Eq. (A-7) the Kraus operators by their partial product expression, we finally obtain $T_1 = \langle g | U_J | g \rangle$, manifesting the invariance of the transformation operators of Eqs. (8)–(9) in the change of Kraus operators. This is the same as $T_1 = \langle g | U'_J | g \rangle = \langle g | U_J | g \rangle$ for any enlarged unitary U'_J since their action on $|g\rangle$ all coincide. In this respect, the specific choice of one set of Kraus operators with associated environment model, among all equivalent sets for channels (1) and (2) as described above, will not change T_1 and T_2 in Eqs. (8)–(9), and therefore will not affect the operation of the superposed channel of Fig. 1. The modeling problem is to have access, for each channel (1) and (2), at least to one convenient pair of Kraus set and environment model, among the infinite number of equivalent pairs, so as to have access to a characterization of the transformation operators T_1 and T_2 of Eqs. (8)–(9) governing the coherent superposition in Fig. 1. This may require, for each channel (1) and (2), beyond a set of Kraus operators, additional knowledge or assumptions concerning the

underlying implementation. Alternatively, in the absence of such constitutive informations or modeling assumptions, an estimation procedure can be envisaged of the unknown channel parameters, as examined in Section 6.4. Besides, in the paper, for qubit channels, we work out a general description having common validity for arbitrary channel parameters.

References

- [1] O. Oreshkov, F. Costa, and Č. Brukner, “Quantum correlations with no causal order,” *Nature Communications*, vol. 3, pp. 1092,1–8, 2012.
- [2] G. Chiribella, G. M. D’Ariano, P. Perinotti, and B. Valiron, “Quantum computations without definite causal structure,” *Physical Review A*, vol. 88, pp. 022318,1–15, 2013.
- [3] D. Ebler, S. Salek, and G. Chiribella, “Enhanced communication with the assistance of indefinite causal order,” *Physical Review Letters*, vol. 120, pp. 120502,1–5, 2018.
- [4] A. A. Abbott, J. Wechs, D. Horsman, M. Mhalla, and C. Branciard, “Communication through coherent control of quantum channels,” *Quantum*, vol. 4, pp. 333,1–14, 2020. (arXiv:1810.09826v3).
- [5] G. Chiribella and H. Kristjánsson, “Quantum Shannon theory with superpositions of trajectories,” *Proceedings of the Royal Society A*, vol. 475, pp. 20180903,1–25, 2019.
- [6] H. Kristjánsson, G. Chiribella, S. Salek, D. Ebler, and M. Wilson, “Resource theories of communication,” *New Journal of Physics*, vol. 22, pp. 073014,1–30, 2020.
- [7] N. Loizeau and A. Grinbaum, “Channel capacity enhancement with indefinite causal order,” *Physical Review A*, vol. 101, pp. 012340,1–6, 2020.
- [8] G. Chiribella, M. Banik, S. S. Bhattacharya, T. Guha, M. Alimuddin, A. Roy, S. Saha, S. Agrawal, and G. Kar, “Indefinite causal order enables perfect quantum communication with zero capacity channels,” *New Journal of Physics*, vol. 23, pp. 033039,1–21, 2021.
- [9] F. Chapeau-Blondeau, “Noisy quantum metrology with the assistance of indefinite causal order,” *Physical Review A*, vol. 103, pp. 032615,1–18, 2021.
- [10] X.-Q. Zhou, T. C. Ralph, P. Kalasuwan, M. Zhang, A. Peruzzo, B. P. Lanyon, and J. L. O’Brien, “Adding control to arbitrary unknown quantum operations,” *Nature Communications*, vol. 2, pp. 413,1–8, 2011.
- [11] M. Friis, V. Dunjko, W. Dür, and H. J. Briegel, “Implementing quantum control for unknown subroutines,” *Physical Review A*, vol. 89, pp. 030303(R),1–5, 2014.
- [12] M. A. Nielsen and I. L. Chuang, *Quantum Computation and Quantum Information*. Cambridge: Cambridge University Press, 2000.
- [13] M. M. Wilde, *Quantum Information Theory*. Cambridge: Cambridge University Press, 2017.
- [14] V. Giovannetti, S. Lloyd, and L. Maccone, “Quantum metrology,” *Physical Review Letters*, vol. 96, pp. 010401,1–4, 2006.
- [15] V. Giovannetti, S. Lloyd, and L. Maccone, “Advances in quantum metrology,” *Nature Photonics*, vol. 5, pp. 222–229, 2011.

- [16] R. Demkowicz-Dobrzański and L. Maccone, “Using entanglement against noise in quantum metrology,” *Physical Review Letters*, vol. 113, pp. 250801,1–4, 2014.
- [17] G. M. D’Ariano, C. Macchiavello, and M. F. Sacchi, “On the general problem of quantum phase estimation,” *Physics Letters A*, vol. 248, pp. 103–108, 1998.
- [18] W. van Dam, G. M. D’Ariano, A. Ekert, C. Macchiavello, and M. Mosca, “Optimal quantum circuits for general phase estimation,” *Physical Review Letters*, vol. 98, pp. 090501,1–4, 2007.
- [19] F. Chapeau-Blondeau, “Optimized probing states for qubit phase estimation with general quantum noise,” *Physical Review A*, vol. 91, pp. 052310,1–13, 2015.
- [20] C. L. Degen, F. Reinhard, and P. Cappellaro, “Quantum sensing,” *Reviews of Modern Physics*, vol. 89, pp. 035002,1–39, 2017.
- [21] H. L. Van Trees, *Detection, Estimation, and Modulation Theory, Part I*. New York: Wiley, 2001.
- [22] S. M. Kay, *Fundamentals of Statistical Signal Processing: Estimation Theory*. Englewood Cliffs: Prentice Hall, 1993.
- [23] T. M. Cover and J. A. Thomas, *Elements of Information Theory*. New York: Wiley, 2006.
- [24] F. Chapeau-Blondeau, “Optimizing qubit phase estimation,” *Physical Review A*, vol. 94, pp. 022334,1–14, 2016.
- [25] O. E. Barndorff-Nielsen and R. D. Gill, “Fisher information in quantum statistics,” *Journal of Physics A*, vol. 33, pp. 4481–4490, 2000.
- [26] M. G. A. Paris, “Quantum estimation for quantum technology,” *International Journal of Quantum Information*, vol. 7, pp. 125–137, 2009.
- [27] M. A. Armen, J. K. Au, J. K. Stockton, A. C. Doherty, and H. Mabuchi, “Adaptive homodyne measurement of optical phase,” *Physical Review Letters*, vol. 89, pp. 133602,1–4, 2002.
- [28] A. Fujiwara, “Strong consistency and asymptotic efficiency for adaptive quantum estimation problems,” *Journal of Physics A*, vol. 39, pp. 12489–12504, 2006.
- [29] D. Brivio, S. Cialdi, S. Vezzoli, B. T. Gebrehiwot, M. G. Genoni, S. Olivares, and M. G. A. Paris, “Experimental estimation of one-parameter qubit gates in the presence of phase diffusion,” *Physical Review A*, vol. 81, pp. 012305,1–7, 2010.
- [30] E. Tesio, S. Olivares, and M. G. A. Paris, “Optimized qubit phase estimation in noisy quantum channels,” *International Journal of Quantum Information*, vol. 9, pp. 379–387, 2011.
- [31] R. Okamoto, M. Iefuji, S. Oyama, K. Yamagata, H. Imai, A. Fujiwara, and S. Takeuchi, “Experimental demonstration of adaptive quantum state estimation,” *Physical Review Letters*, vol. 109, pp. 130404,1–5, 2012.
- [32] W. Larson and B. E. A. Saleh, “Supersensitive ancilla-based adaptive quantum phase estimation,” *Physical Review A*, vol. 96, pp. 042110,1–7, 2017.
- [33] L. Gammaitoni, P. Hänggi, P. Jung, and F. Marchesoni, “Stochastic resonance,” *Reviews of Modern Physics*, vol. 70, pp. 223–287, 1998.

- [34] F. Chapeau-Blondeau, “Noise-assisted propagation over a nonlinear line of threshold elements,” *Electronics Letters*, vol. 35, pp. 1055–1056, 1999.
- [35] M. D. McDonnell, N. G. Stocks, C. E. M. Pearce, and D. Abbott, *Stochastic Resonance: From Suprathreshold Stochastic Resonance to Stochastic Signal Quantization*. Cambridge: Cambridge University Press, 2008.
- [36] F. Duan, F. Chapeau-Blondeau, and D. Abbott, “Weak signal detection: Condition for noise induced enhancement,” *Digital Signal Processing*, vol. 23, pp. 1585–1591, 2013.
- [37] J. J. L. Ting, “Stochastic resonance for quantum channels,” *Physical Review E*, vol. 59, pp. 2801–2803, 1999.
- [38] G. Bowen and S. Mancini, “Stochastic resonance effects in quantum channels,” *Physics Letters A*, vol. 352, pp. 272–275, 2006.
- [39] F. Chapeau-Blondeau, “Qubit state estimation and enhancement by quantum thermal noise,” *Electronics Letters*, vol. 51, pp. 1673–1675, 2015.
- [40] N. Gillard, E. Belin, and F. Chapeau-Blondeau, “Stochastic antiresonance in qubit phase estimation with quantum thermal noise,” *Physics Letters A*, vol. 381, pp. 2621–2628, 2017.
- [41] N. Gillard, E. Belin, and F. Chapeau-Blondeau, “Stochastic resonance with unital quantum noise,” *Fluctuation and Noise Letters*, vol. 18, pp. 1950015,1–15, 2019.
- [42] F. Chapeau-Blondeau, “Optimized entanglement for quantum parameter estimation from noisy qubits,” *International Journal of Quantum Information*, vol. 16, pp. 1850056,1–25, 2018.
- [43] B. Schumacher and M. D. Westmoreland, *Quantum Processes, Systems, and Information*. Cambridge: Cambridge University Press, 2010.